iScience

CellPress
OPEN ACCESS

Article

Virus-Intrinsic Differences and Heterogeneous IRF3 Activation Influence IFN-Independent Antiviral Protection

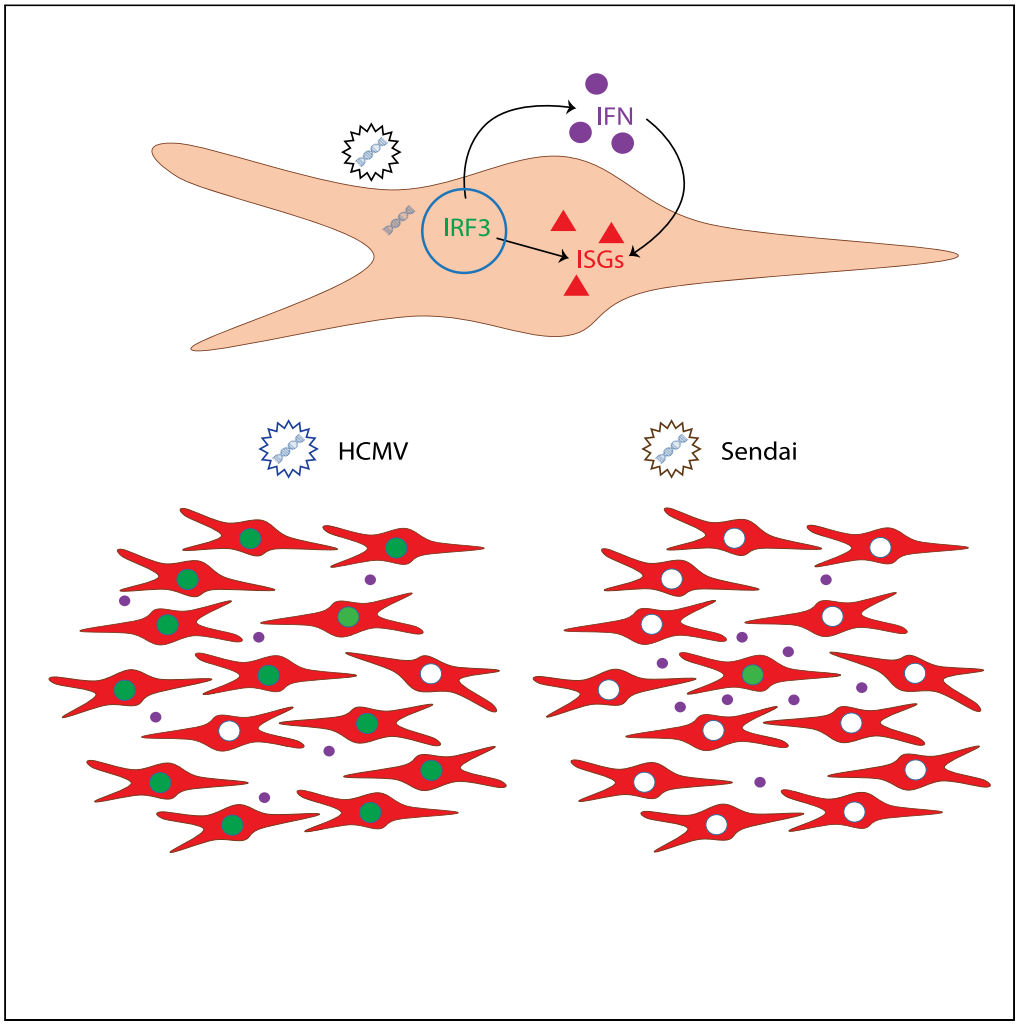

David N. Hare, Kaushal Baid, Anna Dvorkin-Gheva, Karen L. Mossman

mossk@mcmaster.ca

HIGHLIGHTS

The antiviral response to virus particles requires low levels of interferon

Cells respond differently to HCMV or SeV particles

Heterogeneous IRF3 activation influences the response to virus

Hare et al., iScience 23, 101864
December 18, 2020
https://doi.org/10.1016/j.isci.2020.101864

iScience

CellPress
OPEN ACCESS

Article

Virus-Intrinsic Differences and Heterogeneous IRF3 Activation Influence IFN-Independent Antiviral Protection

David N. Hare,[1] Kaushal Baid,[2] Anna Dvorkin-Gheva,[2] and Karen L. Mossman[1,2,*]

SUMMARY

Type 1 interferon (IFN) plays a critical role in early antiviral defense and priming of adaptive immunity by signaling upregulation of host antiviral IFN-stimulated genes (ISGs). Certain stimuli trigger strong activation of IFN regulatory factor 3 (IRF3) and direct upregulation of ISGs in addition to IFN. It remains unclear why some stimuli are stronger activators of IRF3 and how this leads to IFN-independent antiviral protection. We found that UV-inactivated human cytomegalovirus (HCMV) particles triggered an IFN-independent ISG signature that was absent in cells infected with UV-inactivated Sendai virus particles. HCMV particles triggered mostly uniform activation of IRF3 and low-level IFN-β production within the population while SeV particles triggered a small fraction of cells producing abundant IFN-β. These findings suggest that population-level activation of IRF3 and antiviral protection emerges from a diversity of responses occurring simultaneously in single cells. Moreover, this occurs in the absence of virus replication.

INTRODUCTION

Virus infection is sensed by pattern recognition receptors (PRRs) that recognize viral particle components or by-products of replication, such as cytosolic double-stranded RNA (dsRNA) and double-stranded DNA (dsDNA), and upregulate pro-inflammatory and antiviral interferon (IFN)-stimulated genes (ISGs) through production of type 1 IFN. Antiviral ISGs collectively create an antiviral state in infected and surrounding cells to restrict virus spread while pro-inflammatory ISGs recruit immune effector cells. IFN signaling is critical for early control of infection, and productive virus replication is usually dependent on the virus's ability to antagonize IFN signaling (reviewed in (Fensterl and Sen, 2009)).

Both replicating and non-replicating viruses are recognized and contribute to IFN upregulation, but most replicating viruses simultaneously suppress IFN upregulation and signaling. In fact, many viruses trigger stronger IFN responses in the absence of virus gene expression and replication (Collins et al., 2004; Mossman et al., 2001; Preston et al., 2001; Weber et al., 2013). Consequently, the immune response to many important viral pathogens and vaccines is dependent on recognition of defective virus particles or abortive infection (Drayman et al., 2019; Ho et al., 2016; O'Neal et al., 2019; Yount et al., 2006). Recognition of virus particles can involve a combination of stimulatory components, such as viral glycoproteins or packaged nucleic acid, along with cellular perturbations, such as virus entry (Hare et al., 2015; Holm et al., 2012; Juckem et al., 2008). How cells recognize and respond to virus particles are important because these processes play a critical role in the immune response to virus infection, as well as the immune response to non-replicating viral vectors.

IFN-β is the first IFN subtype produced during infection and can be produced by most cell types. The IFN-β promoter contains binding sites for IFN regulatory factors (IRFs), NF-κB and AP1, which together modulate IFN-β expression (reviewed in (Balachandran and Beg, 2011; Honda et al., 2006)). IRF3 is a critical transcription factor for the upregulation of IFN-β and is constitutively expressed in a majority of cells (Au et al., 1995; Hiscott, 2007). When IRF3 is phosphorylated by the kinase tank-binding kinase 1 it undergoes a conformational change that promotes its dimerization, nuclear accumulation, and binding to the IFN-β promoter (Fitzgerald et al., 2003; Lin et al., 1998; Sharma et al., 2003; Yoneyama et al., 1998). Since NF-κB was first observed binding to the IFN-β enhanceosome, it has been shown to be important for early IFN-β upregulation, but it is not essential (Apostolou and Thanos, 2008; Basagoudanavar et al., 2011; Peters et al., 2002).

[1]Pathology and Molecular Medicine, McMaster University, Hamilton, ON L8S4L8, Canada

[2]Biochemistry and Biomedical Sciences, McMaster University, Hamilton, ON L8S4L8, Canada

*Correspondence: mossk@mcmaster.ca

https://doi.org/10.1016/j.isci.2020.101864

After IFN-β is produced and secreted, it binds to the IFN-α/β receptor (IFNAR) on the surface of nearby cells. IFNAR initiates Jak-STAT signaling and formation of a complex containing STAT1, STAT2, and IRF9 named IFN-stimulated gene factor 3 (ISGF3). The ISGF3 complex binds to IFN-stimulated response elements (ISREs) in the promoters of ISGs, thus upregulating hundreds of genes involved in antiviral defense (reviewed in (Schoggins, 2018)).

In addition to upregulating IFN-β, activated IRF3 can directly upregulate a subset of ISGs by binding to ISREs and forming a transcriptional complex with CBP/p300 (Bandyopadhyay et al., 1995; Grandvaux et al., 2002; Weaver et al., 1998). IRF3-mediated upregulation of ISGs is thought to act as a first line of defense to limit virus replication in the infected cell, while IFN-β upregulates ISGs in nearby cells to halt spread of the virus. Low-level infection with non-replicating enveloped virus particles causes IRF3-mediated upregulation of ISGs in the absence of detectable IFN (Collins et al., 2004; Mossman et al., 2001; Paladino et al., 2006). While this response is IRF3-dependent, the extent of observable IRF3 posttranslational modifications fail to correlate with ISG induction (Noyce et al., 2009). Activation of NF-κB and subsequent production of IFN were found to require a higher level of virus particle stimulation (Paladino et al., 2006).

We and others have suggested that non-replicating enveloped virus particles are recognized upon membrane fusion that occurs during virus entry (Collins et al., 2004; Holm et al., 2012; Noyce et al., 2011; Tsitoura et al., 2009). However, we found that sensing of genomic nucleic acid is critical for the antiviral response to low levels of enveloped virus particles (Hare et al., 2015). Given that nucleic acid recognition is known to activate transcription factors necessary for IFN-β production, we revisited the role of IFN-β signaling in the antiviral response to two different enveloped virus particles. Sendai virus (SeV) belongs to the paramyxovirus family and is an enveloped, negative stranded, non-segmented RNA virus. Human cytomegalovirus (HCMV) belongs to the herpesvirus family and is an enveloped dsDNA virus. While SeV and HCMV are known to cause disease in mice and humans, respectively, they are also commonly used models to study innate antiviral pathways.

RESULTS

Fibroblasts Mount an IFN-Independent Antiviral Response to HCMV Particles but Not SeV Particles

While we and others previously described ISG induction in the absence of detectable IFN production, we investigated the role of IFN signaling in the antiviral response to representative enveloped virus particles. We infected wild-type or IFNAR1 KO hTERT-immortalized human fibroblasts (THFs) with either UV-inactivated HCMV (HCMV-UV) or UV-inactivated SeV (SeV-UV) particles and measured the antiviral response. IFNAR1 KO THFs are not responsive to IFN-I but remain capable of mounting IFN-independent antiviral responses to appropriate stimuli. Consistent with previous findings, wild-type THFs infected with low levels of HCMV or SeV particles were protected from vesicular stomatitis virus expressing green fluorescent protein (VSV-GFP) in a plaque reduction assay and IFN was only detected in supernatants after THFs were infected with higher amounts of HCMV or SeV particles. Surprisingly, IFNAR1 KO THFs had a lower antiviral response to HCMV particles, requiring a higher number of particles to achieve full protection (Figure 1A) and IFNAR1 KO THFs did not mount a protective antiviral response to SeV particles at all, regardless of input (Figure 1B). These results suggest that the antiviral response to low levels of HCMV or SeV particles relies on low levels of IFN that are not detected by conventional supernatant transfers. To validate our hypothesis, we concentrated protein in supernatants from wild-type THFs infected with low levels of SeV particles and found that cells treated with these concentrated supernatants were protected (Figure S1).

To further test whether IFN was necessary for the antiviral response to infection with virus particles in wild-type THFs, we blocked IFN signaling with B18R, a recombinant vaccinia virus IFN antagonist (Alcami et al., 2000; Symons et al., 1995), prior to infection with HCMV or SeV particles, and measured the antiviral response using a plaque reduction assay. Similar to IFNAR1 KO THFs, B18R-treated wild-type THFs mounted a protective antiviral response to infection with HCMV particles at high levels of infection but were not protected following infection with SeV particles (Figures 1C and 1D).

IFN-III has been shown to upregulate a similar set of ISGs in cells expressing the IFN-λ receptor (IFNLR) (Kotenko et al., 2003; Sheppard et al., 2003), thus creating a protective antiviral state independent of IFNAR. IFNLR is expressed in cells of epithelial origin but is believed to be absent in fibroblasts. To determine whether THFs respond to IFN-λ, we treated THFs or A549 cells, derived from lung epithelial carcinoma, with

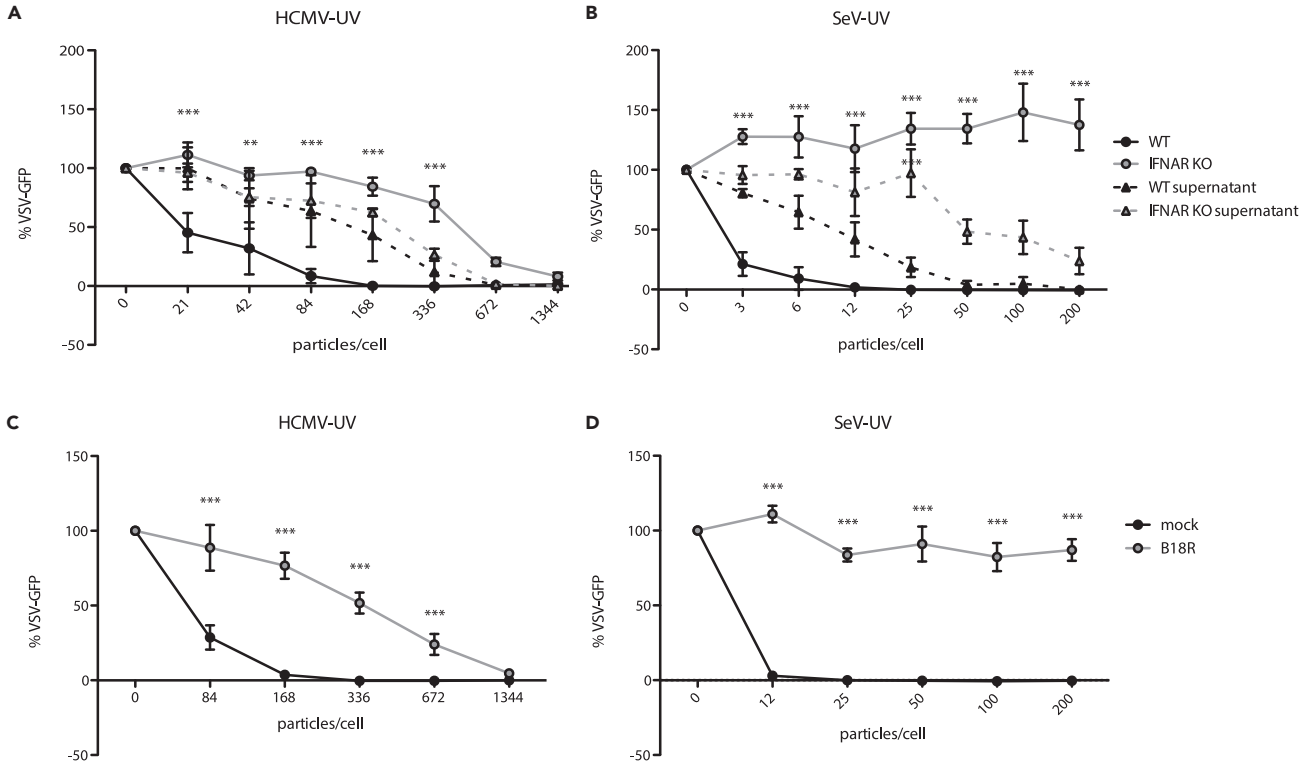

Figure 1. Antiviral Response to HCMV-UV and SeV-UV in the Presence/Absence of IFN Signaling

(A and B) Wild-type (WT) or IFNAR1 KO THFs were infected with increasing levels of UV-inactivated HCMV before challenging with VSV-GFP 16 hr later. The presence of IFN in the supernatants was assayed by transferring supernatants from infected THFs to naive wild-type THFs and challenging them with VSV-GFP 6 hr later (WT supernatant/IFNAR KO supernatant).

(C and D) WT THFs pretreated with B18R or media alone were infected with increasing levels of HCMV-UV or SeV-UV and challenged with VSV-GFP. Mean fluorescence intensity and standard error from 3 biological replicates was plotted as a percentage of mock infected cells challenged with VSV-GFP. WT and IFNAR KO, WT and IFNAR KO supernatant, or mock and B18R treated THFs were compared by two-way analysis of variance (ANOVA) with Bonferroni post-tests (** for $p < 0.01$, *** for $p < 0.001$).

increasing amounts of recombinant IFN-λ1. We found that A549 cells responded to IFN-λ1 in a dose-dependent manner while THFs did not, consistent with THFs lacking IFNLR (Figure S2). Therefore, the antiviral responses we observed in IFNAR1 KO THFs are independent of both IFNAR and IFNLR.

A Subset of IFN-Independent ISGs Are Upregulated in Response to HCMV but Not SeV Particles

Our antiviral data suggested that HCMV particles were capable of stimulating both IFN-independent and IFN-mediated responses while SeV particles only stimulated IFN-mediated responses. To better understand the gene products involved, we employed whole transcriptome sequencing of wild-type or IFNAR1 KO THFs infected with either HCMV-UV or SeV-UV particles. Among genes significantly upregulated >2 fold, IFNAR1 KO THFs infected with HCMV particles upregulated 51% (49/96) of genes upregulated in infected wild-type THFs. In contrast, IFNAR1 KO THFs infected with SeV particles upregulated 6% (5/79) of genes upregulated in infected wild-type THFs. The 30 genes most highly upregulated by either virus had varying degrees of IFN independence in THFs infected with HCMV particles, while there was very little IFN-independent ISG upregulation in THFs infected with SeV particles (Figure 2A). There was a high degree of overlap between all genes significantly upregulated by THFs infected with either virus (Figure 2A and Table S1).

To validate our transcriptome data, we chose two representative ISGs that were mostly IFN independent in THFs infected with HCMV particles but not SeV particles (IFIT1 and ISG15) and one representative ISG whose upregulation was similarly IFN dependent in THFs infected with either virus (CXCL10). Quantitative reverse transcriptase polymerase chain reaction (RT-PCR) findings validated the transcriptomic data for all three genes, following both high- and low-level infection (Figures 2B–2D). The combined transcriptomic

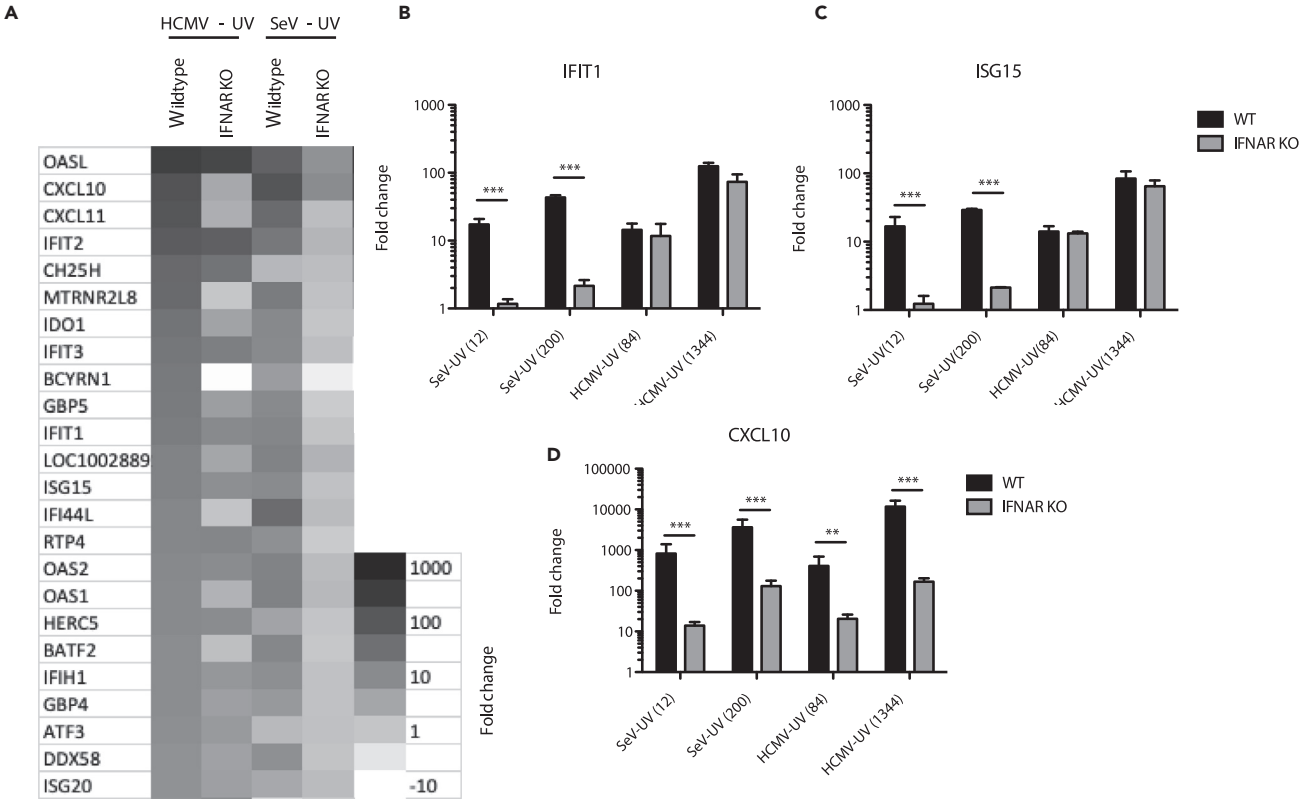

Figure 2. ISG Upregulation in Response to HCMV or SeV Particles

(A) Wild-type (WT) or IFNAR1 KO THFs were treated with 84 particles/cell HCMV-UV or 12 particles/cell SeV-UV and RNA harvested for high-throughput RNA sequencing analysis. The 30 most highly upregulated genes across all samples are shown.

(B–D) WT or IFNAR1 KO THFs were treated with 84 or 1,344 particles/cell of HCMV-UV or 12 or 200 particles/cell of SeV-UV and RNA harvested 6 hr post-treatment. Transcript levels of IFIT1 (B), ISG15 (C), and CXCL10 (D) were measured by quantitative RT-PCR. Mean fold change over mock and standard error from 3-6 biological replicates was graphed and WT and IFNAR KO THFs compared by two-way analysis of variance (ANOVA) with Bonferroni post-tests (** for $p < 0.01$ and *** for $p < 0.001$).

and quantitative RT-PCR results indicate that infection with HCMV particles upregulates a subset of ISGs in an IFN-independent fashion while infection with SeV particles upregulates ISGs almost entirely through IFN-dependent signaling.

IFN-Independent ISG Induction Depends on Cell Type and Virus-Intrinsic Differences

Given that infection with HCMV particles triggers a cyclic GMP-AMP synthase (cGAS)- and stimulator of IFN genes (STING)-dependent antiviral response while SeV particles trigger a mitochondrial antiviral signalling (MAVS)-dependent antiviral response (DeFilippis et al., 2010; Hare et al., 2015; Seth et al., 2005), we hypothesized that dsDNA recognition through STING directly upregulates ISGs more effectively than dsRNA recognition through MAVS. To test this hypothesis, we transfected wild-type and IFNAR1 KO THFs with either dsDNA or dsRNA of a matched 1,000 base pair sequence and harvested cellular RNA 6 hr later. Transfection with either dsDNA or dsRNA was sufficient to upregulate IFIT1, ISG15, and CXCL10 in IFNAR1 KO THFs (Figures 3A–3C).

Next, we chose to test whether the differences in IFN-independent responses between HCMV and SeV particles also held true between replicating HCMV and SeV. Under similar experimental conditions, ISG induction to replicating HCMV (Figures 3D–3F) mirrored that of non-replicating HCMV (Figures 2B–2D), while ISG induction by replicating SeV (Figures 3D–3F) more closely mirrored that of transfected dsRNA (Figures 3A–3C) as opposed to SeV-UV (Figures 2C–2E). Thus, IFIT1 and ISG15 upregulation by SeV is less IFN dependent than what we observed with SeV-UV. Moreover, similar to UV-inactivated particles, there are clear differences in the antiviral response to replicating HCMV or SeV.

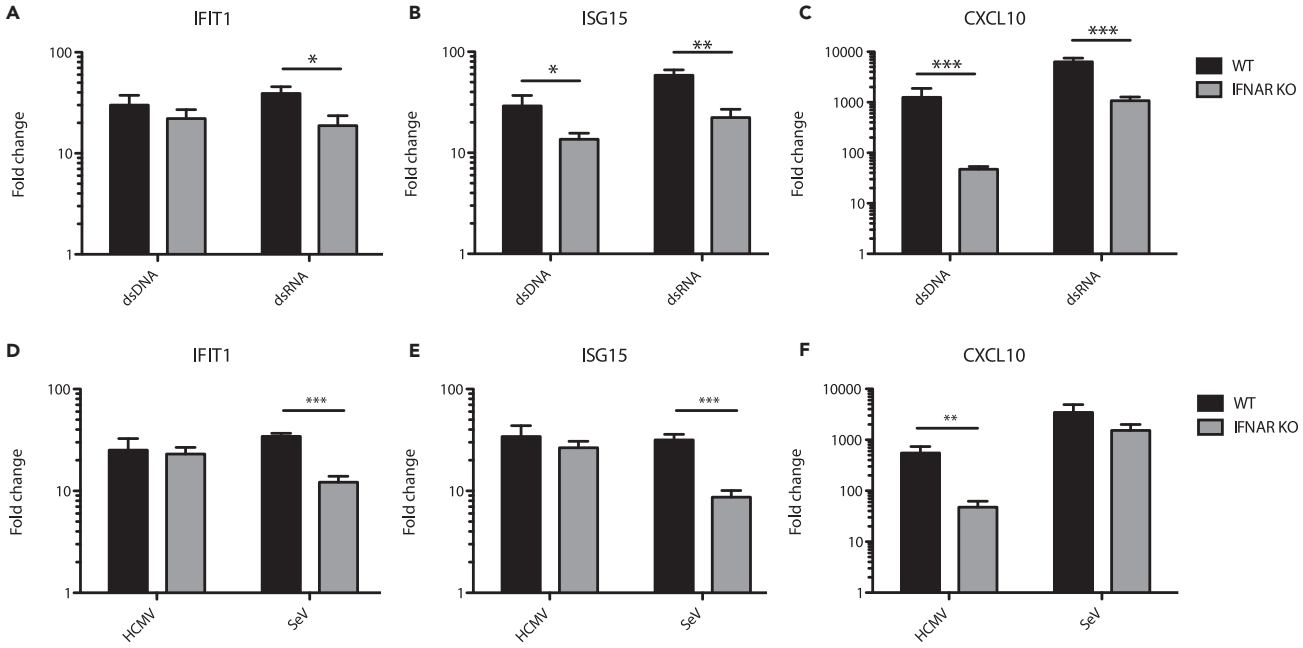

Figure 3. ISG Upregulation in Response to Transfected Nucleic Acid or Replicating Virus

Wild-type (WT) or IFNAR1 KO THFs were transfected with matched sequence dsRNA or dsDNA (A–C) or infected with replication competent HCMV or SeV and RNA harvested 6 hr post-treatment (D–F). Transcript levels of IFIT1 (A and D), ISG15 (B and E), and CXCL10 (C and F) were measured by quantitative RT-PCR. Mean fold change over mock and standard error from 3-7 biological replicates was graphed and WT and IFNAR KO THFs compared by two-way analysis of variance (ANOVA) with Bonferroni post-tests (* for $p < 0.05$, ** for $p < 0.01$ and *** for $p < 0.001$).

To determine whether different cell types similarly upregulate ISGs through IFN-dependent and cell-intrinsic pathways, we infected THFs and a variety of primary and immortalized cells with low levels of SeV-UV or HCMV-UV. To measure ISG transcript upregulation in the absence of IFN production, we used the inhibitor cycloheximide (CHX) to block *de novo* protein synthesis. Consistent with cell-intrinsic IFN-independent signaling, HCMV-UV infection strongly upregulated IFIT1 and ISG15 transcripts in THFs and primary human embryonic lung (HEL) fibroblasts in the absence of protein synthesis (Figures 4A–4F). As expected, IFN-independent upregulation of ISGs in THFs and HEL fibroblasts was significantly lower following SeV-UV infection (Figures 4A–4F). Immortalized bronchiole epithelial cells (NuLi-1) responded similarly to SeV-UV but not at all when infected with HCMV-UV (Figures 4G–4I), consistent with a previous report of impaired entry of HCMV strain AD169 in epithelial cells (Ryckman et al., 2006). Interestingly, THP-1-derived macrophages upregulated IFIT1 and ISG15 in the absence of protein synthesis following infection with SeV-UV instead of HCMV-UV (Figures 4J–4L). This may be because THP-1 macrophages have higher basal expression of nucleic acid sensors, as we observed in preliminary experiments (data not shown). Thus, both fibroblasts and macrophages appear to upregulate ISGs through both IFN-dependent and cell-intrinsic pathways, with differences noted between RNA and DNA viruses.

HCMV and SeV Particles Differentially Activate IRF3

We previously demonstrated that IRF3 is essential for the antiviral response to a variety of enveloped virus particles and that activation of RelA, a subunit of NF-κB, is associated with a higher level of particle stimulation and detectable IFN-β production (Collins et al., 2004; Paladino et al., 2006). The involvement of IFN signaling prompted us to re-examine the relative contribution of these two transcription factors in THFs treated with either HCMV or SeV particles.

To test the relative importance of IRF3 and NF-κB, we infected wild-type, IRF3 KO, or RelA KO THFs with increasing levels of HCMV or SeV particles and measured antiviral responses, IFN production, and upregulation of representative ISGs. Consistent with previous findings, IRF3 was essential for antiviral protection (Figures 5A and 5B), IFN production (Figures 5C and 5D), and upregulation of IFIT1, ISG15, and CXCL10 (Figures 5E–5G) in response to infection with either HCMV or SeV particles. RelA was dispensable for

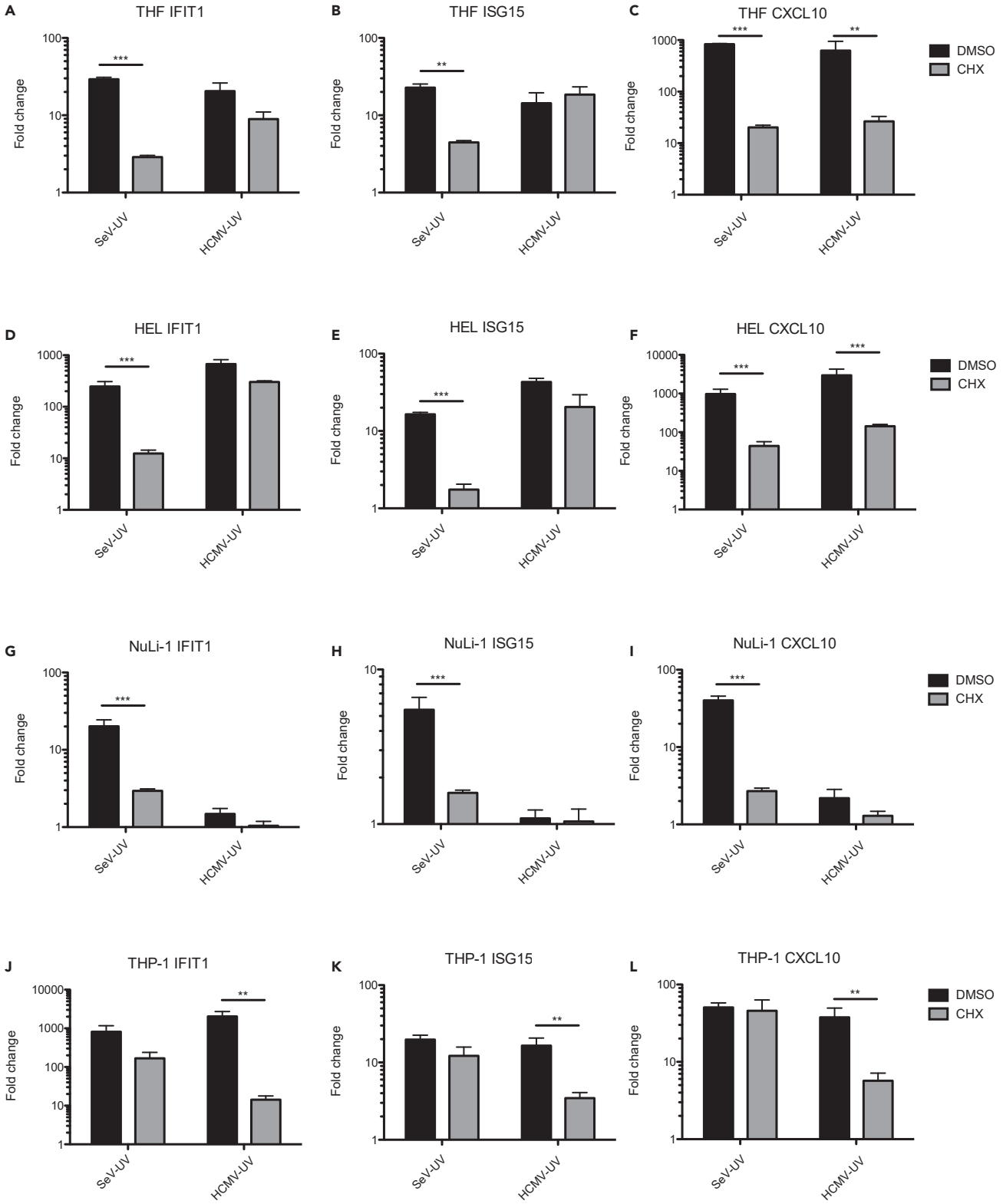
A
THF IFIT1
B
THF ISG15
C
THF CXCL10
D
HEL IFIT1
E
HEL ISG15
F
HEL CXCL10
G
NuLi-1 IFIT1
H
NuLi-1 ISG15
I
NuLi-1 CXCL10
J
THP-1 IFIT1
K
THP-1 ISG15
L
THP-1 CXCL10
Fold change
SeV-UV
HCMV-UV
DMSO
CHX

Figure 4. ISG Upregulation in Different Cell Types Infected with HCMV and SeV Particles

(A–L) THFs (A–C), HEL fibroblasts (D–F), NuLi-1 epithelial cells (G–I), or THP-1-derived macrophages (J–L) were infected with 84 particles/cell HCMV or 12 particles/cell SeV in the presence of the protein synthesis inhibitor CHX or DMSO alone and RNA harvested 6 hr post-treatment. Transcript levels of IFIT1, ISG15, and CXCL10 were measured by quantitative RT-PCR. Mean fold change over mock and standard error from 3-4 biological replicates was graphed and DMSO- and CHX-treated cells compared by two-way analysis of variance (ANOVA) with Bonferroni post-tests (** for $p < 0.01$ and *** for $p < 0.001$).

antiviral protection, IFN production, and upregulation of ISGs after treatment with HCMV particles but did play a role in response to SeV particles (Figures 5A–5G).

Given the importance of IRF3 for the antiviral response to infection with either HCMV or SeV particles, we measured IRF3 activation in wild-type THFs infected with either HCMV or SeV particles. We observed IRF3 nuclear translocation in the majority of cells following infection with HCMV particles but only in a small proportion of THFs infected with SeV particles (Figures 5H and 5I). Collectively, these data suggest that SeV particles may trigger an IRF3-dependent IFN response in a minority of cells that protects the monolayer through paracrine signaling. By virtue of HCMV particles stimulating IRF3 more evenly across the monolayer, cells are less reliant on paracrine IFN signaling for antiviral protection.

HCMV and SeV Particles Induce Heterogeneous IFN-β Production

To measure IFN-β production in individual cells, we generated THFs with a stably integrated green fluorescent protein (GFP) reporter controlled by the IFN-β promoter sequence (IFN-β-GFP THFs). We used flow cytometry to measure upregulation of GFP (IFN-β) and ISG15 in our IFN-β-GFP THF reporter line. IFN-β-GFP THFs treated with 1000 U/ml recombinant IFNα had increased ISG15 expression but no change in GFP (Figure 6A). Infection with HCMV particles increased GFP expression in the majority of cells and increased ISG15 expression in nearly all cells. Infection with SeV particles increased GFP expression in <5% of cells but increased ISG15 expression in nearly all cells.

To determine the contribution of IFN signaling to ISG15 expression in individual cells, we pretreated IFN-β-GFP THFs with B18R prior to infection with HCMV or SeV particles to block IFN signaling (but not production). As expected, ISG15 upregulation by recombinant IFNα was nearly absent when IFN-β-GFP THFs were pretreated with B18R (Figure 6A). When IFN-β-GFP THFs were infected with either HCMV or SeV particles, pre-treatment with B18R primarily prevented ISG15 upregulation in cells lacking GFP upregulation. This observation is consistent with ISG15^{high} GFP^{high} cells upregulating ISG15 directly, while ISG15^{high} GFP^{low} cells upregulate ISG15 through IFN-dependent signaling.

To confirm our flow cytometry data and better visualize cell populations, we observed GFP (IFN-β) and ISG15 in adherent IFN-β-GFP THFs using immunofluorescence microscopy. As with flow cytometry, GFP was upregulated in the majority of cells treated with HCMV particles and highly upregulated in <5% of cells treated with SeV particles, with ISG15 observed throughout both treated populations (Figure 6B). Similar to our flow cytometry data, treatment with B18R predominantly affected ISG15 expression in SeV particle treated cells and predominantly in cells lacking IFNβ production.

The simplest explanation for heterogeneous IFN-β production in THFs infected with SeV-UV is that IFN-β producing THFs contain more SeV particles. We infected IFN-β-GFP THFs with replicating SeV or SeV-UV, measured SeV proteins using a pan-specific SeV antibody and were able to detect SeV protein in both SeV and SeV-UV infected IFN-β-GFP THFs. However, we found no clear correlation between GFP expression and SeV protein in IFN-β-GFP THFs infected with SeV particles (Figure 7A). SeV is known to produce and package defective viral genomes (DVGs) recognized by RIG-I during SeV infection, and these may be responsible for IFN-β production in cells infected with SeV particles (Baum et al., 2010; Sanchez-Aparicio et al., 2017). We infected IFN-β-GFP THFs with SeV particles and sorted GFP^{high} and GFP^{low} cells before harvesting RNA. We measured both genomic SeV (gSeV) and SeV DVG-546, the predominant DVG found in the SeV stocks used in this study, using quantitative RT-PCR with primers designed by *Genoyer, et al.* (Genoyer and Lopez, 2019). We detected gSeV and DVG-546 in GFP^{high} and GFP^{low} cells but found no difference in gSeV and a noticeable but not significant increase in DVG-546 in GFP^{high} cells (Figures 7B and 7C).

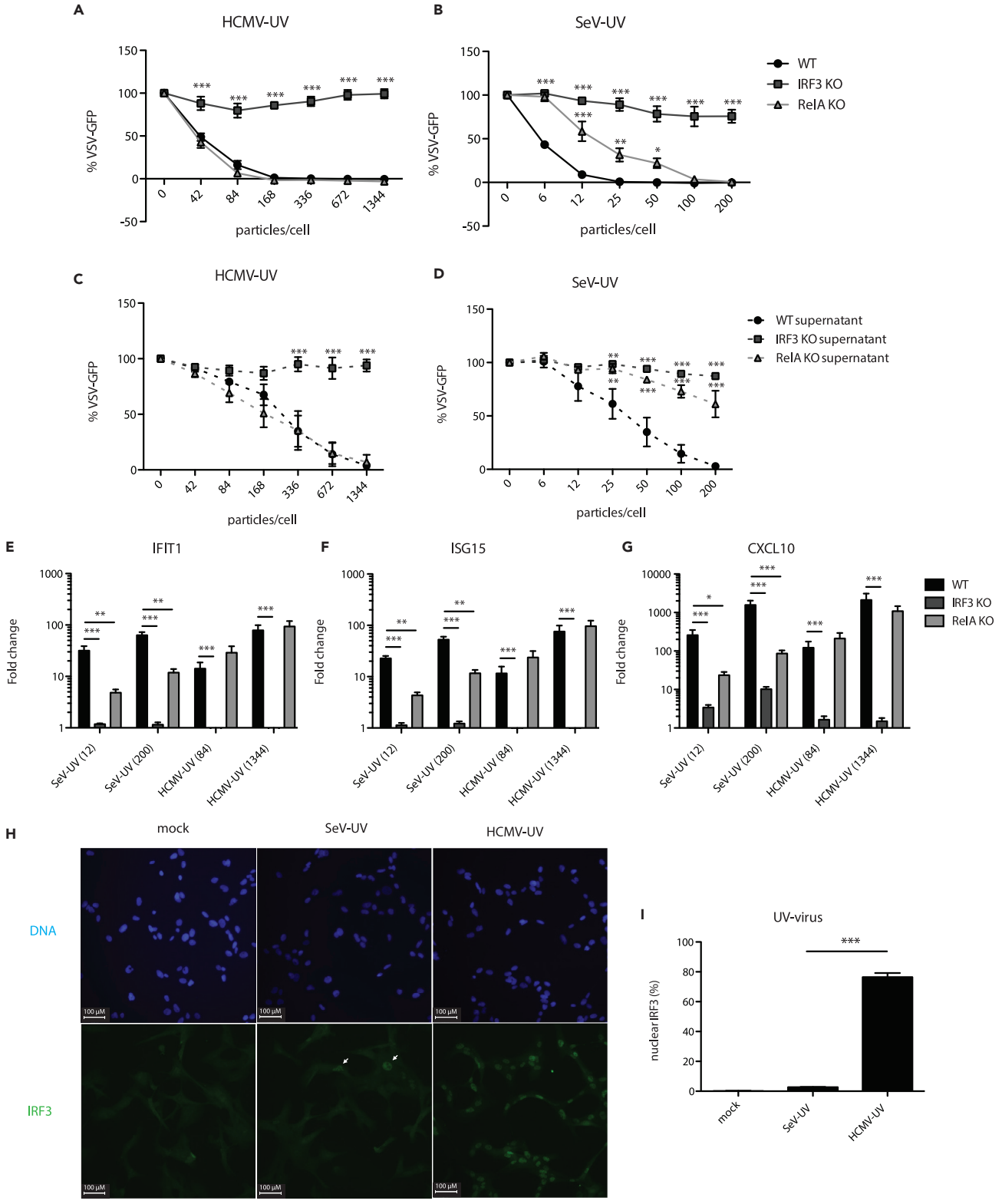
A
HCMV-UV
% VSV-GFP
particles/cell
B
SeV-UV
WT
IRF3 KO
RelA KO
C
HCMV-UV
D
SeV-UV
WT supernatant
IRF3 KO supernatant
RelA KO supernatant
E
IFIT1
F
ISG15
G
CXCL10
Fold change
SeV-UV (12)
SeV-UV (200)
HCMV-UV (84)
HCMV-UV (1344)
H
mock
SeV-UV
HCMV-UV
DNA
IRF3
100 μM
I
UV-virus
nuclear IRF3 (%)

Figure 5. Role of IRF3 and RelA in the Antiviral Response to HCMV and SeV Particles

(A–D) Wild-type (WT), IRF3 KO, or RelA KO THFs were treated with increasing levels of UV-inactivated HCMV or SeV (A and B), and 16 hr post-treatment supernatants were transferred to naive WT THFs (C and D). All THFs were subsequently challenged with VSV-GFP. Mean GFP fluorescence and standard error from 3 biological replicates were plotted as a percentage of mock treated, VSV-GFP infected cells. IRF3 and RelA KO THFs were compared with wild type by two-way analysis of variance (ANOVA) with Bonferroni post-tests (* for $p < 0.05$, ** for $p < 0.01$ and *** for $p < 0.001$).

(E–G) WT, IRF3, or RelA KO THFs were treated with 84 or 1,344 particles/cell of HCMV-UV or 12 or 200 particles/cell of SeV-UV and transcript levels of IFIT1, ISG15, and CXCL10 were measured by quantitative RT-PCR. Mean fold change relative to mock and standard error from 7 biological replicates was graphed. IRF3 and RelA KO THFs were compared with wild type by two-way ANOVA with Bonferroni post-tests (* for $p < 0.05$, ** for $p < 0.01$ and *** for $p < 0.001$).

(H) WT THFs were treated with 1,344 particles/cell of HCMV-UV or 200 particles/cell of SeV-UV, fixed 4 hr post-treatment and IRF3 and cell nuclei visualized by immunofluorescence microscopy. Scale bars of 100 μm are shown, and IRF3 +ve nuclei in SeV-UV infected THFs are marked.

(I) IRF3-positive nuclei as a percentage of total nuclei were calculated from 3 independent fields of view and mean % IRF3 positive nuclei and standard error from 3 biological replicates were graphed. SeV-UV and HCMV-UV infected THFs were compared by student's t-test (*** for $p < 0.001$).

DISCUSSION

Our previous reporting of an IRF3-dependent IFN-independent response to incoming virus particles stemmed from examination of individual ISGs by RT-PCR and an inability in multiple assays to detect IFN (Collins et al., 2004; Mossman et al., 2001). Similar to other studies, our early interpretation was that membrane perturbation during virus entry, independent of subsequent virus replication or the need for viral genomes, stimulates a similar response to all enveloped virus particles (Collins et al., 2004; Holm et al., 2012; Noyce et al., 2011). Along with previous findings (Hare et al., 2015), this study clearly demonstrates a difference in the cellular response to HCMV and SeV particles, despite both being enveloped virus particles. Although HCMV and SeV contain DNA and RNA genomes, respectively, differential nucleic acid sensing alone does not explain the differences in the antiviral response to each, as THFs responded similarly to transfected dsRNA and dsDNA.

Consistent with previous studies, HCMV particles induced IRF3-mediated upregulation of ISGs. Unexpectedly, low levels of HCMV particles also induced IRF3-mediated upregulation of IFN. It is difficult to determine the relative contribution of IFN-dependent versus IFN-independent ISG upregulation to antiviral defense in wild-type cells, as IRF3 is essential for both IFN-β production and direct ISG upregulation in this system. While IFNAR1 KO cells upregulate an IRF3-dependent subset of ISGs that are protective against subsequent challenge, a higher level of particle stimulation is required for full protection. Therefore, it appears that IFN-β and IRF3 upregulate complimentary and overlapping sets of ISGs that act in concert to protect cells from infection.

In contrast to HCMV, we found that SeV particles strongly stimulate a minority of cells that protect the surrounding monolayer through production of IFN-β. Heterogeneous production of IFN-β has been described in response to several different replicating viruses, even following high multiplicity or *in vivo* infection (Chen et al., 2010; Drayman et al., 2019; Kallfass et al., 2013; Killip et al., 2017; O'Neal et al., 2019; Rand et al., 2012; Zawatzky et al., 1985). In many of these cases, IFN-β production occurs in abortively infected cells where the virus fails to suppress antiviral signaling (Drayman et al., 2019; O'Neal et al., 2019). The percentage of IFN-β producing cells varies widely among viruses and infected cell types and results from a combination of virus- and cell-intrinsic factors (Killip et al., 2017; Rand et al., 2012; Zhao et al., 2012).

We found SeV genomes and defective viral genomes in cells regardless of whether they were producing IFN-β. While SeV defective viral genomes contain complimentary ends that form stimulatory dsRNA recognized by RIG-I, packaged SeV defective genomes are normally tightly bound by nucleocapsid protein which prevent formation of the stimulatory hairpin structure (Kolakofsky, 1976). However, not all SeV genomes may be properly packaged in nucleoprotein owing to errors in replication exacerbated by the presence of defective genomes (Genoyer and Lopez, 2019). This additional requirement may explain why only a small fraction of cells infected with SeV particles produced IFN-β. Unfortunately, we were not able to measure whether SeV genomes and SeV DVG-546 were exposed in all SeV-UV infected cells or only in a subset. However, it appears that delivery of packaged SeV RNA is insufficient for recognition by RIG-I, and additional factors are required for immune activation.

While in this study we used HCMV and SeV as representative DNA and RNA viruses, respectively, we do not propose that all enveloped DNA or RNA viruses will respond in a similar fashion. Indeed, the diversity of responses is likely to mirror the diverse composition of different virus particles. As the innate antiviral response to virus infection is heavily dependent on recognition of non-replicating virus particles,

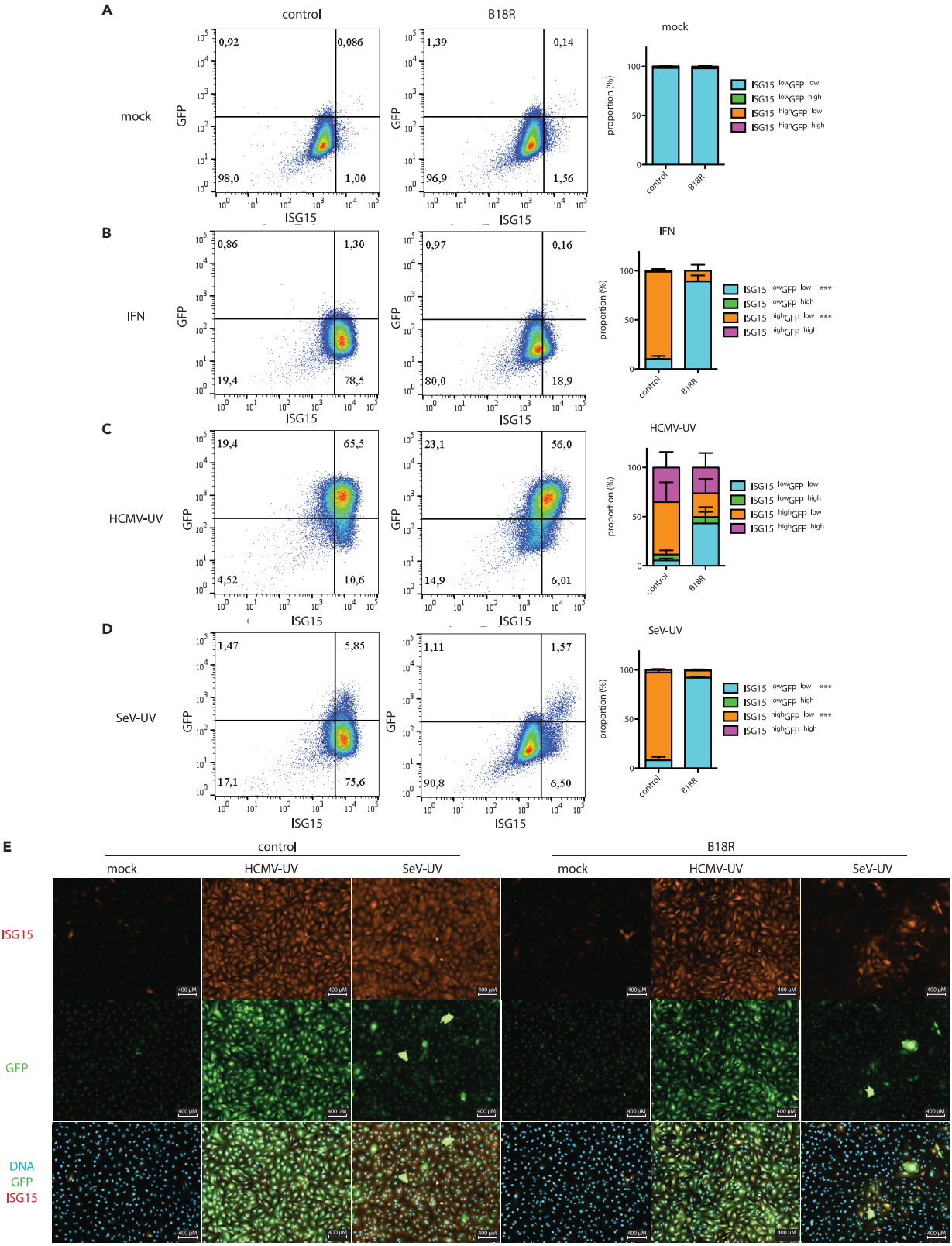
A
control
B18R
mock
GFP
ISG15
0,92
0,086
98,0
1,00
1,39
0,14
96,9
1,56
mock
proportion (%)
control
B18R
ISG15 lowGFP low
ISG15 lowGFP high
ISG15 highGFP low
ISG15 highGFP high
B
IFN
0,86
1,30
19,4
78,5
0,97
0,16
80,0
18,9
IFN
***
C
HCMV-UV
19,4
65,5
4,52
10,6
23,1
56,0
14,9
6,01
HCMV-UV
D
SeV-UV
1,47
5,85
17,1
75,6
1,11
1,57
90,8
6,50
SeV-UV
E
control
B18R
mock
HCMV-UV
SeV-UV
ISG15
GFP
DNA
GFP
ISG15
400 μM

Figure 6. Single-Cell Dynamics of IFN-β and ISG15 Upregulation in Response to HCMV or SeV Particles

(A–E) IFN-β-GFP THFs were pretreated with B18R or media alone and mock treated, treated with IFNα (1000 U/ml), infected with HCMV-UV (1,344 particles/cell), or infected with SeV-UV (200 particles/cell). Cells were fixed 16 hr later and levels of GFP and ISG15 expression measured by flow cytometry (A–D). Cells were categorized as $GFP^{low/high}$ and $ISG15^{low/high}$ based on measurements of mock treated cells and mean proportion and standard error from 3 biological replicates graphed. Similarly, treated IFN-β-GFP THFs were visualized by fluorescence microscopy, and representative images from 3 biological replicates are shown (E). Scale bars of 400 μm are shown.

understanding intrinsic and innate responses to diverse infections helps explain why some infections are associated with greater disease. Moreover, understanding the innate response to non-replicating virus particles is becoming more important as virus-based therapies engineered in the lab make their way to the clinic. Introducing genes by *in vivo* or *ex vivo* transduction of cells relies on minimizing the innate response to virus vectors to maximize engraftment and stable expression of therapeutic genes (Brown et al., 2007). In contrast, viral vaccines or oncolytic virus require a robust innate response in order to recruit and activate antigen-presenting cells (Davola and Mossman, 2019; Proietti et al., 2002; Walsh et al., 2019). Notably, SeV is being developed as a vector for gene therapy, as well as vaccination, and the ability to modulate immunogenicity of SeV particles will be important for either application (reviewed in (Baltusnikas et al., 2019; Nakanishi and Otsu, 2012; Saga and Kaneda, 2015)). Lipid-based delivery of nucleic acid is used in addition to virus-based vectors and also triggers innate immune activation. Our results suggest that formulation and delivery route for nucleic acid may influence the innate response as much as the nucleic acid itself and must be taken into account.

Limitations of the Study

The experiments described in this study were done in life-extended human fibroblasts with HCMV and SeV used as representative enveloped viruses. Fibroblasts are often used as a model system in which to study regulation of IFN-β, sometimes referred to as fibroblast IFN, because they play an important role in the first

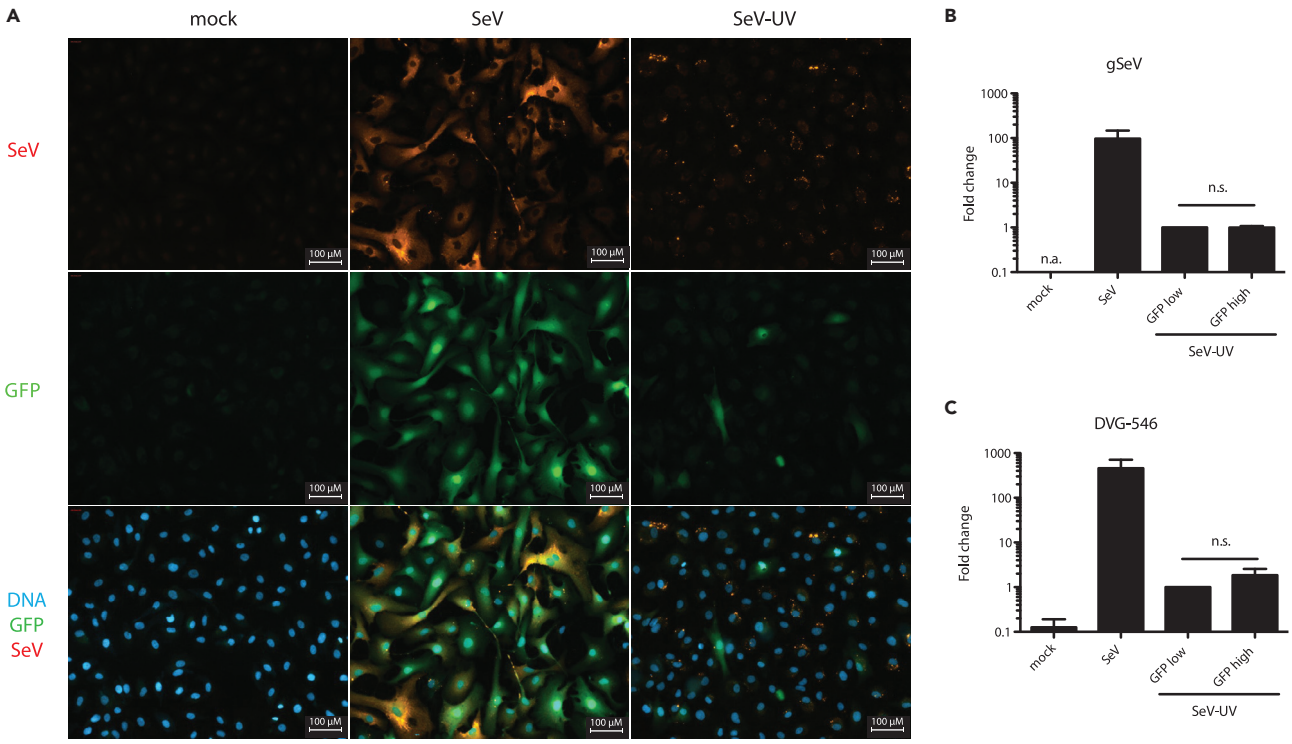

Figure 7. Relative SeV Abundance in IFN-β Producing Cells

(A–C) IFN-β-GFP THFs were mock infected, infected with replicating SeV (200 particles/cell), or infected with SeV-UV (200 particles/cell). (A) Cells were fixed 16 hr later and GFP and SeV proteins visualized by fluorescence microscopy. Scale bars of 100 μm are shown. (B and C) SeV-UV infected cells were sorted for GFP fluorescence 16 hr post-infection and gSeV (B) or DVG-546 (C) measured by quantitative RT-PCR. Mean fold change relative to SeV-UV-GFP^{low} and standard error from 3 biological replicates was graphed. SeV-UV-GFP^{low} and SeV-UV-GFP^{high} populations were compared by student's t-test. n.a., no amplification; n.s., not significant.

wave of IFN-β production during infection. Although nearly all cells are capable of producing and responding to IFN-β, there is some variation in signaling pathways present across different cell types. It remains to be seen how heterogeneous IFN-β production affects antiviral protection in tissue made up of many different cell types. HCMV and SeV are both well-studied enveloped viruses in the context of innate immune activation and seem to activate a dramatically different proportion of cells. These results show that differences may exist in the antiviral response to non-replicating virus particles, but further experiments with other virus particles are necessary to understand what type of innate response they induce.

Resource Availability

Lead Contact

Further information and requests for resources and reagents should be directed to and will be fulfilled by the lead contact, Karen L Mossman (mossk@mcmaster.ca).

Materials Availability

All unique/stable reagents generated in this study are available from the Lead Contact with a completed Materials Transfer Agreement.

Data and Code Availability

The RNA-seq data generated during this study are available at GEO (GEO: GSE149705).

METHODS

All methods can be found in the accompanying Transparent Methods supplemental file.

SUPPLEMENTAL INFORMATION

Supplemental Information can be found online at https://doi.org/10.1016/j.isci.2020.101864.

ACKNOWLEDGMENTS

We would like to thank Dr. Victor DeFilippis for providing us with hTERT-immortalized human fibroblasts (THF) and various knock-out lines used in this study. D.H. was supported by a Natural Sciences and Engineering Research Council of Canada (NSERC) doctoral scholarship and through the Ontario Graduate Scholarship program. Studies in the Mossman Lab were supported by a Canadian Institutes of Health Research (CIHR) project grant (MOP 57669).

AUTHOR CONTRIBUTIONS

D.H. and K.M. conceived and designed the study. D.H. and K.B. performed experiments. A.D.-G. analyzed transcriptome data. D.H. and K.M. wrote the paper.

DECLARATION OF INTERESTS

The authors declare no competing interests.

Received: March 24, 2020
Revised: May 4, 2020
Accepted: November 20, 2020
Published: December 18, 2020

REFERENCES

Alcami, A., Symons, J.A., and Smith, G.L. (2000). The vaccinia virus soluble alpha/beta interferon (IFN) receptor binds to the cell surface and protects cells from the antiviral effects of IFN. J. Virol. *74*, 11230–11239.

Apostolou, E., and Thanos, D. (2008). Virus Infection Induces NF-kappaB-dependent interchromosomal associations mediating monoallelic IFN-beta gene expression. Cell *134*, 85–96.

Au, W.C., Moore, P.A., Lowther, W., Juang, Y.T., and Pitha, P.M. (1995). Identification of a member of the interferon regulatory factor family that binds to the interferon-stimulated response element and activates expression of interferon-induced genes. Proc. Natl. Acad. Sci. U S A *92*, 11657–11661.

Balachandran, S., and Beg, A.A. (2011). Defining emerging roles for NF-kappaB in antivirus responses: revisiting the interferon-beta enhanceosome paradigm. PLoS Pathog. *7*, e1002165.

Baltusnikas, J., Satkauskas, S., and Lundstrom, K. (2019). Constructing RNA viruses for long-term transcriptional gene silencing. Trends Biotechnol. *37*, 20–28.

Bandyopadhyay, S.K., Leonard, G.T., Jr., Bandyopadhyay, T., Stark, G.R., and Sen, G.C. (1995). Transcriptional induction by double-stranded RNA is mediated by interferon-stimulated response elements without activation of interferon-stimulated gene factor 3. J. Biol. Chem. *270*, 19624–19629.

Basagoudanavar, S.H., Thapa, R.J., Nogusa, S., Wang, J., Beg, A.A., and Balachandran, S. (2011). Distinct roles for the NF-kappa B RelA subunit during antiviral innate immune responses. J. Virol. *85*, 2599–2610.

Baum, A., Sachidanandam, R., and Garcia-Sastre, A. (2010). Preference of RIG-I for short viral RNA molecules in infected cells revealed by next-generation sequencing. Proc. Natl. Acad. Sci. U S A *107*, 16303–16308.

Brown, B.D., Sitia, G., Annoni, A., Hauben, E., Sergi, L.S., Zingale, A., Roncarolo, M.G., Guidotti, L.G., and Naldini, L. (2007). In vivo administration of lentiviral vectors triggers a type I interferon response that restricts hepatocyte gene transfer and promotes vector clearance. Blood *109*, 2797–2805.

Chen, S., Short, J.A., Young, D.F., Killip, M.J., Schneider, M., Goodbourn, S., and Randall, R.E. (2010). Heterocellular induction of interferon by negative-sense RNA viruses. Virology *407*, 247–255.

Collins, S.E., Noyce, R.S., and Mossman, K.L. (2004). Innate cellular response to virus particle entry requires IRF3 but not virus replication. J. Virol. *78*, 1706–1717.

Davola, M.E., and Mossman, K.L. (2019). Oncolytic viruses: how "lytic" must they be for therapeutic efficacy? Oncoimmunology *8*, e1581528.

DeFilippis, V.R., Alvarado, D., Sali, T., Rothenburg, S., and Fruh, K. (2010). Human cytomegalovirus induces the interferon response via the DNA sensor ZBP1. J. Virol. *84*, 585–598.

Drayman, N., Patel, P., Vistain, L., and Tay, S. (2019). HSV-1 single-cell analysis reveals the activation of anti-viral and developmental programs in distinct sub-populations. Elife *8*, e46339.

Fensterl, V., and Sen, G.C. (2009). Interferons and viral infections. Biofactors *35*, 14–20.

Fitzgerald, K.A., McWhirter, S.M., Faia, K.L., Rowe, D.C., Latz, E., Golenbock, D.T., Coyle, A.J., Liao, S.M., and Maniatis, T. (2003). IKKepsilon and TBK1 are essential components of the IRF3 signaling pathway. Nat. Immunol. *4*, 491–496.

Genoyer, E., and Lopez, C.B. (2019). Defective viral genomes alter how Sendai virus interacts with cellular trafficking machinery, leading to heterogeneity in the production of viral particles among infected cells. J. Virol. *93*, e01579–18.

Grandvaux, N., Servant, M.J., tenOever, B., Sen, G.C., Balachandran, S., Barber, G.N., Lin, R., and Hiscott, J. (2002). Transcriptional profiling of interferon regulatory factor 3 target genes: direct involvement in the regulation of interferon-stimulated genes. J. Virol. *76*, 5532–5539.

Hare, D.N., Collins, S.E., Mukherjee, S., Loo, Y.M., Gale, M., Jr., Janssen, L.J., and Mossman, K.L. (2015). Membrane perturbation-associated Ca2+ signalling and incoming genome sensing are required for the host response to low-level enveloped virus particle entry. J. Virol. *90*, 3018–3027.

Hiscott, J. (2007). Triggering the innate antiviral response through IRF-3 activation. J. Biol. Chem. *282*, 15325–15329.

Ho, T.H., Kew, C., Lui, P.Y., Chan, C.P., Satoh, T., Akira, S., Jin, D.Y., and Kok, K.H. (2016). PACT- and RIG-I-dependent activation of type I interferon production by a defective interfering RNA derived from measles virus vaccine. J. Virol. *90*, 1557–1568.

Holm, C.K., Jensen, S.B., Jakobsen, M.R., Cheshenko, N., Horan, K.A., Moeller, H.B., Gonzalez-Dosal, R., Rasmussen, S.B., Christensen, M.H., Yarovinsky, T.O., et al. (2012). Virus-cell fusion as a trigger of innate immunity dependent on the adaptor STING. Nat. Immunol. *13*, 737–743.

Honda, K., Takaoka, A., and Taniguchi, T. (2006). Type I interferon [corrected] gene induction by the interferon regulatory factor family of transcription factors. Immunity *25*, 349–360.

Juckem, L.K., Boehme, K.W., Feire, A.L., and Compton, T. (2008). Differential initiation of innate immune responses induced by human cytomegalovirus entry into fibroblast cells. J. Immunol. *180*, 4965–4977.

Kallfass, C., Lienenklaus, S., Weiss, S., and Staeheli, P. (2013). Visualizing the beta interferon response in mice during infection with influenza A viruses expressing or lacking nonstructural protein 1. J. Virol. *87*, 6925–6930.

Killip, M.J., Jackson, D., Perez-Cidoncha, M., Fodor, E., and Randall, R.E. (2017). Single-cell studies of IFN-beta promoter activation by wild-type and NS1-defective influenza A viruses. J. Gen. Virol. *98*, 357–363.

Kolakofsky, D. (1976). Isolation and characterization of sendai virus DI-RNAs. Cell *8*, 547–555.

Kotenko, S.V., Gallagher, G., Baurin, V.V., Lewis-Antes, A., Shen, M., Shah, N.K., Langer, J.A., Sheikh, F., Dickensheets, H., and Donnelly, R.P. (2003). IFN-lambdas mediate antiviral protection through a distinct class II cytokine receptor complex. Nat. Immunol. *4*, 69–77.

Lin, R., Heylbroeck, C., Pitha, P.M., and Hiscott, J. (1998). Virus-dependent phosphorylation of the IRF-3 transcription factor regulates nuclear translocation, transactivation potential, and proteasome-mediated degradation. Mol. Cell Biol. *18*, 2986–2996.

Mossman, K.L., Macgregor, P.F., Rozmus, J.J., Goryachev, A.B., Edwards, A.M., and Smiley, J.R. (2001). Herpes simplex virus triggers and then disarms a host antiviral response. J. Virol. *75*, 750–758.

Nakanishi, M., and Otsu, M. (2012). Development of Sendai virus vectors and their potential applications in gene therapy and regenerative medicine. Curr. Gene Ther. *12*, 410–416.

Noyce, R.S., Collins, S.E., and Mossman, K.L. (2009). Differential modification of interferon regulatory factor 3 following virus particle entry. J. Virol. *83*, 4013–4022.

Noyce, R.S., Taylor, K., Ciechonska, M., Collins, S.E., Duncan, R., and Mossman, K.L. (2011). Membrane perturbation elicits an IRF3-dependent, interferon-independent antiviral response. J. Virol. *85*, 10926–10931.

O'Neal, J.T., Upadhyay, A.A., Wolabaugh, A., Patel, N.B., Bosinger, S.E., and Suthar, M.S. (2019). West nile virus-inclusive single-cell RNA sequencing reveals heterogeneity in the type I interferon response within single cells. J. Virol. *93*, e01778–18.

Paladino, P., Cummings, D.T., Noyce, R.S., and Mossman, K.L. (2006). The IFN-independent response to virus particle entry provides a first line of antiviral defense that is independent of TLRs and retinoic acid-inducible gene I. J. Immunol. *177*, 8008–8016.

Peters, K.L., Smith, H.L., Stark, G.R., and Sen, G.C. (2002). IRF-3-dependent, NFkappa B- and JNK-independent activation of the 561 and IFN-beta genes in response to double-stranded RNA. Proc. Natl. Acad. Sci. U S A *99*, 6322–6327.

Preston, C.M., Harman, A.N., and Nicholl, M.J. (2001). Activation of interferon response factor-3 in human cells infected with herpes simplex virus type 1 or human cytomegalovirus. J. Virol. *75*, 8909–8916.

Proietti, E., Bracci, L., Puzelli, S., Di Pucchio, T., Sestili, P., De Vincenzi, E., Venditti, M., Capone, I., Seif, I., De Maeyer, E., et al. (2002). Type I IFN as a natural adjuvant for a protective immune response: lessons from the influenza vaccine model. J. Immunol. *169*, 375–383.

Rand, U., Rinas, M., Schwerk, J., Nohren, G., Linnes, M., Kroger, A., Flossdorf, M., Kaly-Kullai, K., Hauser, H., Hofer, T., et al. (2012). Multi-layered stochasticity and paracrine signal propagation shape the type-I interferon response. Mol. Syst. Biol. *8*, 584.

Ryckman, B.J., Jarvis, M.A., Drummond, D.D., Nelson, J.A., and Johnson, D.C. (2006). Human cytomegalovirus entry into epithelial and endothelial cells depends on genes UL128 to UL150 and occurs by endocytosis and low-pH fusion. J. Virol. *80*, 710–722.

Saga, K., and Kaneda, Y. (2015). Oncolytic Sendai virus-based virotherapy for cancer: recent advances. Oncolytic Virother. *4*, 141–147.

Sanchez-Aparicio, M.T., Garcin, D., Rice, C.M., Kolakofsky, D., Garcia-Sastre, A., and Baum, A. (2017). Loss of Sendai virus C protein leads to accumulation of RIG-I immunostimulatory defective interfering RNA. J. Gen. Virol. *98*, 1282–1293.

Schoggins, J.W. (2018). Recent advances in antiviral interferon-stimulated gene biology. F1000Res. *7*, 309.

Seth, R.B., Sun, L., Ea, C.K., and Chen, Z.J. (2005). Identification and characterization of MAVS, a mitochondrial antiviral signaling protein that activates NF-kappaB and IRF 3. Cell *122*, 669–682.

Sharma, S., tenOever, B.R., Grandvaux, N., Zhou, G.P., Lin, R., and Hiscott, J. (2003). Triggering the interferon antiviral response through an IKK-related pathway. Science *300*, 1148–1151.

Sheppard, P., Kindsvogel, W., Xu, W., Henderson, K., Schlutsmeyer, S., Whitmore, T.E., Kuestner, R., Garrigues, U., Birks, C., Roraback, J., et al. (2003). IL-28, IL-29 and their class II cytokine receptor IL-28R. Nat. Immunol. *4*, 63–68.

Symons, J.A., Alcami, A., and Smith, G.L. (1995). Vaccinia virus encodes a soluble type I interferon receptor of novel structure and broad species specificity. Cell *81*, 551–560.

Tsitoura, E., Thomas, J., Cuchet, D., Thoinet, K., Mavromara, P., and Epstein, A.L. (2009). Infection with herpes simplex type 1-based amplicon vectors results in an IRF3/7-dependent, TLR-independent activation of the innate antiviral response in primary human fibroblasts. J. Gen. Virol. *90*, 2209–2220.

Walsh, S.R., Bastin, D., Chen, L., Nguyen, A., Storbeck, C.J., Lefebvre, C., Stojdl, D., Bramson, J.L., Bell, J.C., and Wan, Y. (2019). Type I IFN blockade uncouples immunotherapy-induced antitumor immunity and autoimmune toxicity. J. Clin. Invest. *129*, 518–530.

Weaver, B.K., Kumar, K.P., and Reich, N.C. (1998). Interferon regulatory factor 3 and CREB-binding protein/p300 are subunits of double-stranded RNA-activated transcription factor DRAF1. Mol. Cell Biol. *18*, 1359–1368.

Weber, M., Gawanbacht, A., Habjan, M., Rang, A., Borner, C., Schmidt, A.M., Veitinger, S., Jacob, R., Devignot, S., Kochs, G., et al. (2013). Incoming RNA virus nucleocapsids containing a 5′-triphosphorylated genome activate RIG-I and antiviral signaling. Cell Host Microbe *13*, 336–346.

Yoneyama, M., Suhara, W., Fukuhara, Y., Fukuda, M., Nishida, E., and Fujita, T. (1998). Direct triggering of the type I interferon system by virus infection: activation of a transcription factor complex containing IRF-3 and CBP/p300. EMBO J. *17*, 1087–1095.

Yount, J.S., Kraus, T.A., Horvath, C.M., Moran, T.M., and Lopez, C.B. (2006). A novel role for viral-defective interfering particles in enhancing dendritic cell maturation. J. Immunol. *177*, 4503–4513.

Zawatzky, R., De Maeyer, E., and De Maeyer-Guignard, J. (1985). Identification of individual interferon-producing cells by in situ hybridization. Proc. Natl. Acad. Sci. U S A *82*, 1136–1140.

Zhao, M., Zhang, J., Phatnani, H., Scheu, S., and Maniatis, T. (2012). Stochastic expression of the interferon-beta gene. PLoS Biol. *10*, e1001249.

iScience, Volume *23*

Supplemental Information

Virus-Intrinsic Differences and Heterogeneous IRF3 Activation Influence IFN-Independent Antiviral Protection

David N. Hare, Kaushal Baid, Anna Dvorkin-Gheva, and Karen L. Mossman

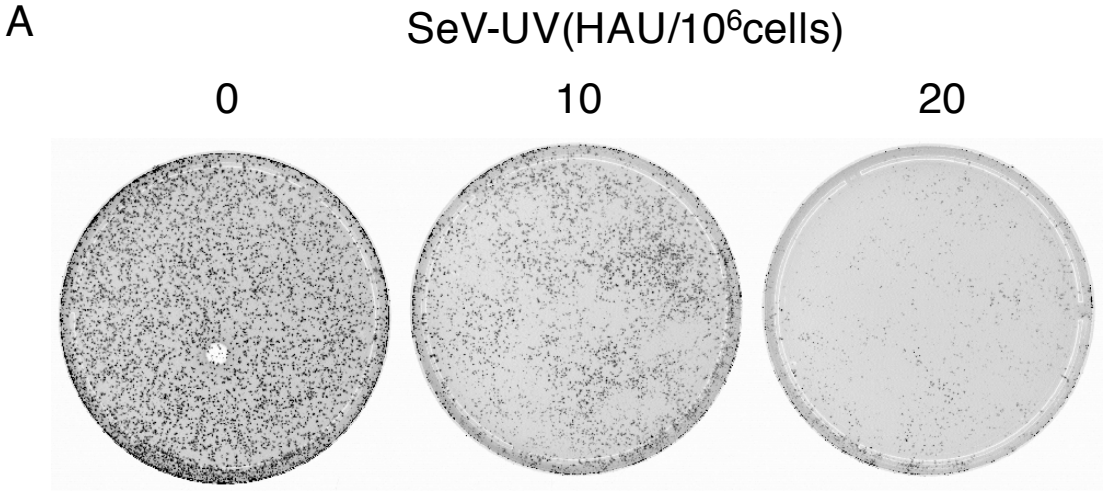

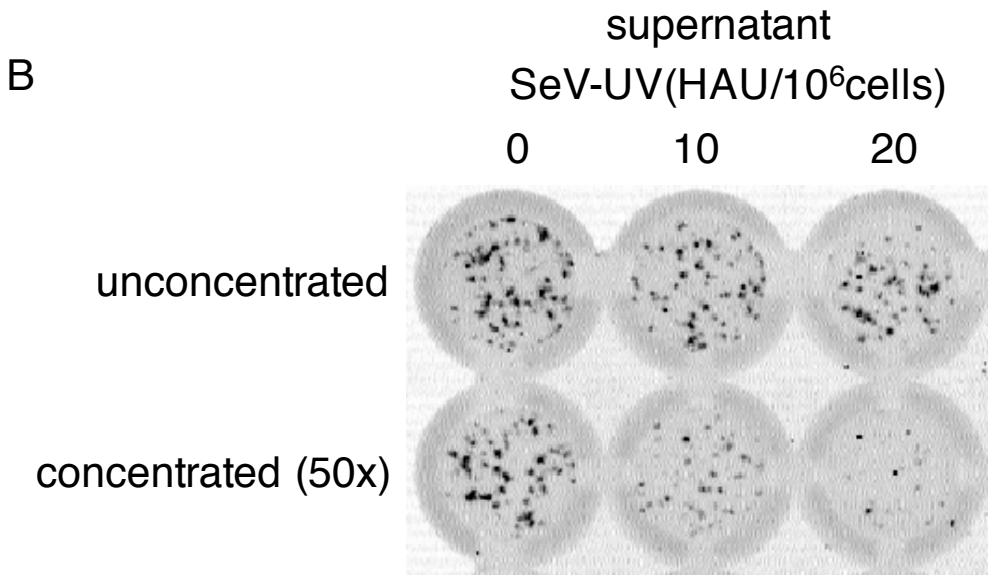

Supplementary figure 1 - IFN detected in concentrated supernatants from SeV-UV infected THFs (Related to Figure 1). 1 x 10^6 THFs were treated with the indicated amount of SeV-UV and incubated for 16 hours before concentrating the supernatant 50-fold and transferring concentrated or non-concentrated supernatants in 100 µl to 1 x 10^4 THFs and performing a plaque reduction assay. THFs were challenged with VSV-GFP either 16 hours after SeV-UV treatment (A) or 6 hours after supernatant transfer (B).

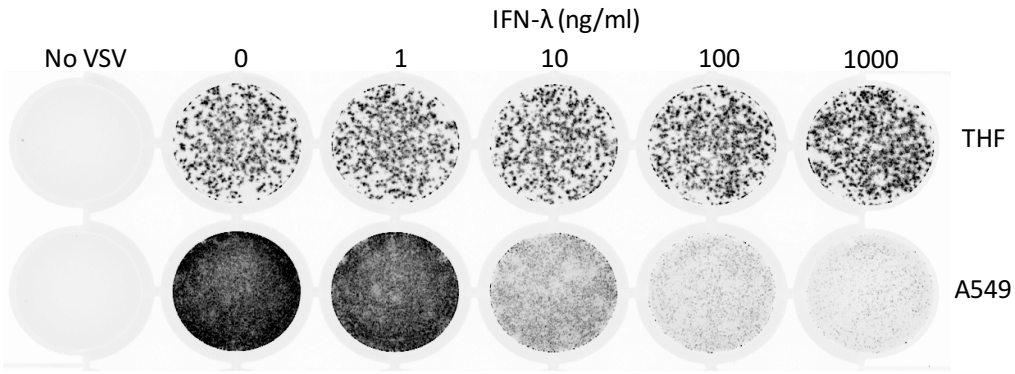

Supplementary figure 2 - A549 but not THFs protected following treatment with recombinant IFN-λ (Related to Figure 1). THFs or A549 were treated with the indicated concentration of IFN-λ and challenged with VSV-GFP 6 hours later in a plaque reduction assay.

Supplementary Table 1 - Differential expression of genes significantly upregulated in HCMV-UV or SeV-UV treated wildtype or IFNAR1 KO THFs (Related to Figure 2)

Gene	Fold change				Gene	Fold change			
	wildtype		IFNAR KO			wildtype		IFNAR KO	
	HCMV-UV	SeV-UV	HCMV-UV	SeV-UV		HCMV-UV	SeV-UV	HCMV-UV	SeV-UV
OASL	**303.44**	**64.35**	**215.92**	7.28	RNF19B	**1.52**	**1.53**	1.13	1.05
CXCL10	**120.79**	**112.51**	2.89	**9.60**	SLFN5	**1.51**	**2.31**	1.16	1.14
CXCL11	**109.44**	**42.17**	2.33	1.40	LAP3	**1.51**	**1.68**	1.01	-1.05
IFIT2	**85.17**	**21.80**	**72.92**	1.83	RGAG1	1.50	-1.33	**2.06**	1.07
CH25H	**46.06**	1.73	**27.37**	1.37	SOX13	**1.50**	1.04	1.24	-1.05
IDO1	**27.33**	**11.02**	3.66	1.00	TMEM126A	**1.50**	1.09	-1.15	1.09
IFIT3	**24.11**	**10.90**	**16.89**	1.30	SERPINB2	**1.49**	**1.61**	1.20	1.35
GBP5	**19.69**	**10.79**	**4.39**	-1.23	SKIDA1	1.48	1.30	**2.09**	1.29
IFIT1	**18.69**	**12.57**	**10.90**	1.11	VSIG10L	1.48	**1.61**	-1.07	-1.05
LOC100288911	**14.45**	**14.57**	3.26	2.03	OGFR	**1.48**	**1.76**	1.10	1.02
ISG15	**14.33**	**9.91**	**8.28**	1.21	XKR8	**1.47**	1.07	1.29	1.07
IFI44L	**12.17**	**39.63**	1.05	1.43	RPS6KC1	**1.46**	1.08	1.31	1.08
RTP4	**12.01**	**7.75**	**12.47**	-1.20	FAM26E	**1.46**	1.10	1.34	1.03
OAS2	**10.95**	**13.91**	**9.80**	1.44	ELF1	**1.45**	**1.48**	1.09	1.02
OAS1	**10.66**	**14.83**	**2.00**	1.66	STAT2	**1.45**	**1.85**	1.27	1.08
HERC5	**10.25**	**3.48**	**9.66**	1.03	RASGRP3	1.44	**1.87**	-1.10	-1.09
BATF2	**9.38**	**12.16**	1.28	-1.09	DDX60L	**1.44**	**2.43**	1.07	-1.12
IFIH1	**9.26**	**8.05**	**6.11**	1.18	APOBEC3G	1.43	**1.69**	1.21	1.28
GBP4	**9.17**	**5.42**	**4.03**	1.13	FNDC3A	**1.43**	1.09	1.23	1.06
ATF3	**8.21**	1.57	**5.31**	1.22	LCP2	**1.43**	-1.00	1.24	1.11
DDX58	**7.57**	**7.70**	**3.94**	1.11	TMEM38A	**1.43**	1.12	-1.06	**-1.45**
ISG20	**7.15**	**2.93**	**4.01**	1.43	TMEM51	**1.42**	1.05	1.19	-1.03
CD7	**6.23**	**2.85**	1.43	-1.40	HMOX1	1.42	1.65	1.50	**1.78**
AIM2	**6.08**	2.00	**4.10**	-3.02	ZBTB42	**1.41**	**1.48**	-1.03	-1.02
XAF1	**5.99**	**11.98**	1.29	1.23	DNAJB5	**1.41**	-1.09	1.25	-1.08
IFI44	**5.93**	**4.98**	**6.65**	1.30	SP100	**1.41**	**1.83**	-1.00	-1.04
RARRES3	**5.93**	1.18	**3.04**	-1.17	LYSMD2	**1.40**	1.33	-1.08	-1.16
THEMIS2	**5.83**	**6.74**	1.60	-1.87	RP6-109B7.3	**1.39**	-1.08	1.05	1.15
CD48	**5.65**	2.35	1.38	1.35	TBXA2R	**1.39**	1.14	-1.02	1.02
USP18	**5.65**	**8.37**	1.87	-1.26	TMEM62	**1.39**	**1.39**	1.02	1.06
RHEBL1	**5.63**	1.39	**4.15**	-1.02	KLF9	**1.38**	1.27	**1.44**	**1.44**
NFKBIZ	**5.41**	1.37	**4.53**	1.03	MTERFD3	**1.38**	1.11	-1.23	-1.07
DDX60	**5.28**	**3.08**	**3.44**	-1.01	WARS	**1.37**	1.23	1.10	1.07
TNFSF10	**5.26**	**6.41**	1.75	1.39	IFITM3	**1.37**	**1.40**	1.03	1.05
NCF2	**5.07**	1.07	**2.33**	-1.38	KIAA0040	**1.37**	1.24	1.06	1.01
IRF1	**4.94**	**2.89**	**1.89**	1.08	PRKD2	**1.37**	**1.70**	1.07	1.06
HELZ2	**4.63**	**8.05**	1.11	1.17	PHF11	1.36	**1.73**	1.01	-1.00
KLF4	**4.58**	1.24	**2.91**	-1.07	B4GALT5	**1.36**	1.02	1.14	-1.01
MX2	**4.49**	**7.86**	**1.58**	1.02	GBP3	**1.36**	**1.48**	1.08	1.04
RANBP3L	**4.26**	-1.10	1.19	-1.03	PNPT1	1.36	**2.22**	1.00	1.00
IL6	**3.93**	1.15	**9.44**	1.95	GTPBP1	**1.36**	1.23	1.21	1.00
SNPH	**3.90**	1.06	**3.00**	-1.06	FENDRR	**1.36**	1.17	**1.39**	1.13
HERC6	**3.75**	**3.06**	**2.21**	-1.03	MASTL	**1.35**	**1.61**	1.01	-1.01
ZC3HAV1	**3.67**	**2.44**	**2.55**	1.06	GCA	**1.35**	1.20	-1.17	-1.10
SAMD9	**3.62**	**3.96**	**1.67**	1.00	BTN3A3	**1.34**	1.16	-1.04	-1.03
CEACAM1	**3.49**	1.70	**2.44**	1.07	IFNAR2	**1.34**	1.03	1.13	-1.08
ADAP1	**3.43**	-1.12	**2.50**	1.26	TRIM56	**1.33**	**1.57**	1.18	1.03
SLC15A3	**3.39**	**4.68**	1.47	1.22	RBM43	1.33	**1.52**	1.07	1.06
APOL6	**3.35**	**2.88**	**2.37**	1.10	FBXO30	**1.33**	1.05	**1.44**	1.17
DTX3L	**3.31**	**4.57**	1.22	-1.04	ZNF107	**1.33**	**1.41**	1.12	1.09
DHX58	**3.27**	**2.97**	**2.52**	1.10	ADAR	**1.33**	**1.71**	1.01	-1.02
PTGS2	**3.24**	1.14	1.21	1.42	CASP7	**1.33**	**1.52**	1.00	1.02
NEDD9	**3.15**	1.15	**2.16**	-1.05	MCL1	**1.32**	1.18	1.25	-1.00

IFI6	**3.13**	**3.84**	1.34	1.01	FAM76A	**1.32**	**1.36**	1.28	1.23
KRT17	**3.11**	1.78	1.45	1.06	GALM	**1.31**	1.09	-1.03	-1.01
PMAIP1	**3.09**	1.19	**2.44**	-1.05	STAMBPL1	**1.31**	-1.20	1.21	-1.06
APOL1	**3.09**	**1.87**	**2.31**	1.09	CNP	**1.30**	**1.37**	1.00	-1.01
TMEM229B	**3.02**	**1.83**	**2.26**	1.00	TMEM219	**1.30**	1.10	1.13	-1.05
PARP9	**2.95**	**4.90**	1.17	-1.09	BTN3A1	**1.30**	1.15	1.13	1.01
TMEM140	**2.93**	**2.97**	1.81	1.18	MOB3C	**1.30**	**1.43**	-1.01	1.06
IFITM1	**2.80**	**4.16**	1.24	-1.40	MAP4K4	**1.30**	-1.00	**1.22**	-1.01
MX1	**2.80**	**4.53**	1.38	1.02	IL1R1	**1.30**	1.07	**1.32**	1.09
FAM46A	**2.77**	**1.83**	**1.63**	-1.01	COX7B2	**1.30**	1.21	-1.00	1.03
DAPP1	2.68	**3.54**	1.21	1.21	CYTH1	**1.29**	**1.37**	1.05	-1.07
GRIP2	**2.63**	1.71	1.58	1.07	TRIM22	1.29	**1.97**	1.13	-1.02
ZNF43	**2.62**	1.47	2.25	1.10	RNF31	**1.29**	**1.49**	1.07	-1.01
IFIT5	**2.60**	**2.88**	1.21	-1.05	SHISA5	**1.29**	**1.28**	1.02	-1.00
ZNFX1	**2.57**	**2.47**	**1.88**	1.06	OBFC1	**1.28**	-1.06	1.08	1.05
APOL2	**2.56**	**1.75**	**1.89**	1.08	TAF8	**1.27**	1.09	**1.30**	1.10
CCRN4L	**2.53**	1.15	**2.22**	1.10	BCL2L13	**1.27**	**1.32**	-1.03	1.04
PLEKHA4	**2.52**	**2.38**	1.52	-1.03	SERTAD1	**1.27**	**1.29**	1.06	1.11
PLSCR1	**2.50**	**3.81**	1.01	-1.12	CCDC6	**1.27**	1.03	1.15	-1.06
PTGER4	**2.48**	1.08	1.81	-1.09	BLZF1	1.27	**1.50**	-1.08	-1.01
PARP10	**2.37**	**3.65**	1.19	1.08	TIPARP	**1.26**	1.20	**1.29**	1.22
IRF9	**2.37**	**3.02**	1.13	1.07	UBA7	1.26	**1.63**	-1.04	1.01
SECTM1	**2.37**	**1.86**	1.33	1.09	DCP1A	**1.26**	**1.40**	1.13	1.09
G0S2	**2.35**	1.29	1.44	1.19	PCGF5	**1.25**	1.11	1.08	1.00
TRIM21	**2.33**	**2.68**	1.10	1.01	PANX1	**1.25**	**1.21**	1.14	1.01
LOC102724224	**2.32**	1.89	1.37	1.03	PLEKHA3	**1.25**	1.05	1.07	-1.02
SAMD9L	**2.29**	**3.26**	**1.40**	1.08	PHACTR4	1.25	**1.38**	1.09	1.03
ASPHD2	**2.27**	1.37	**1.60**	1.09	LGALS3BP	**1.24**	**1.24**	1.02	-1.01
REC8	**2.24**	**2.71**	1.09	1.26	COA6	**1.24**	1.14	-1.04	1.06
USP32P1	2.23	**3.20**	1.88	1.34	GPBP1	**1.23**	1.19	1.14	1.06
APOL3	**2.22**	**1.89**	**2.05**	-1.10	ASNA1	**1.23**	1.05	-1.05	-1.01
NRG2	**2.22**	1.44	1.15	1.09	PELO	**1.23**	1.02	1.11	1.08
FGF2	**2.21**	1.01	**2.26**	1.05	PSME2	**1.23**	**1.22**	-1.01	1.04
ZFP36L2	**2.18**	1.03	**2.11**	1.03	SPATS2L	**1.23**	1.19	1.05	-1.02
PARP14	**2.18**	**3.64**	**1.48**	1.20	MLKL	1.22	**1.56**	1.00	1.10
PPM1K	**2.17**	**2.07**	**1.77**	1.06	CHMP5	**1.22**	**1.29**	-1.03	-1.02
PARP12	**2.16**	**2.80**	1.04	-1.10	SLC35C2	**1.22**	1.08	-1.00	-1.03
TRANK1	**2.15**	**2.08**	**1.98**	1.01	GCLM	1.21	1.20	1.17	**1.29**
BAMBI	**2.09**	-1.00	**2.41**	1.04	B2M	**1.21**	1.09	-1.01	-1.06
NEURL1	**2.08**	**1.83**	1.24	1.30	PSME1	**1.20**	**1.18**	1.03	-1.01
RNF149	**2.07**	1.12	**1.65**	1.06	SLC2A13	**1.20**	1.09	1.08	1.04
SOCS1	**2.04**	**1.69**	1.05	1.08	PRDX2	**1.20**	1.08	1.11	1.00
TNFAIP3	**2.04**	1.06	**1.75**	1.02	DNAJA1	**1.20**	**1.22**	1.02	-1.01
SLC25A28	**2.02**	**2.39**	-1.02	1.04	MRPL22	**1.20**	1.16	**-1.19**	-1.10
FAM65B	**2.02**	1.11	-1.00	1.02	SHOX2	1.20	**1.45**	-1.03	1.05
TRPC4	**2.00**	1.01	1.20	-1.01	TRIM5	1.20	**1.53**	1.08	1.12
SP110	**1.97**	**2.95**	1.06	-1.09	ATP5SL	**1.20**	1.09	-1.01	-1.03
OAS3	**1.97**	**2.71**	1.17	1.02	FMR1	1.19	**1.26**	1.09	-1.00
GBP1	**1.95**	**2.29**	1.09	1.01	GPR180	1.18	**1.32**	1.04	1.10
PIK3AP1	**1.93**	1.40	1.38	1.23	EHD4	1.18	**1.36**	1.07	1.01
GMPR	**1.92**	**2.93**	1.32	1.23	TRIQK	**1.18**	1.05	1.04	1.03
ZCCHC2	**1.92**	**2.37**	1.09	1.08	RBCK1	1.18	**1.30**	1.07	1.01
COL24A1	**1.92**	**2.00**	-1.12	1.13	STAMBP	**1.18**	1.05	-1.05	-1.01
LOC102724927	**1.91**	1.62	-1.08	-1.15	NUP54	**1.18**	1.08	-1.05	-1.03
SAMHD1	**1.91**	**2.40**	1.17	-1.03	SPCS1	**1.16**	1.06	-1.04	-1.02
UBE2L6	**1.91**	**2.16**	1.25	1.11	CMTR1	1.16	**1.39**	1.05	-1.01
ARID5A	**1.90**	1.47	1.14	-1.22	HOXD10	1.16	**1.28**	-1.04	-1.08
LOC728769	**1.88**	1.62	1.02	-1.09	ETS2	1.16	**1.39**	-1.06	1.01
HES4	**1.87**	1.78	1.50	-1.15	CCDC113	1.16	1.04	1.92	**2.60**

TRIM14	**1.85**	**2.55**	1.25	1.03	GTPBP2	1.16	**1.41**	-1.04	1.01
N4BP1	**1.84**	**1.90**	1.25	1.04	FHL3	**1.15**	1.10	-1.10	-1.05
CD274	**1.82**	**1.65**	1.12	-1.07	DUSP16	1.14	**1.29**	1.13	-1.00
TLR3	1.82	**2.44**	-1.19	1.04	TNFRSF21	1.14	1.05	**1.27**	1.07
BST2	**1.81**	**2.12**	1.11	1.04	SEMA3A	1.14	-1.07	**1.53**	-1.03
MYD88	**1.81**	**2.46**	-1.05	-1.08	IER2	1.13	**1.29**	-1.13	-1.05
TRIM25	**1.80**	**2.57**	-1.02	1.01	MED25	1.12	**1.20**	1.05	-1.07
SIX2	**1.79**	1.11	1.32	-1.35	ZNF844	1.12	**1.47**	1.10	1.01
C19orf66	**1.79**	**2.64**	1.00	1.04	KIAA0226	1.11	**1.24**	1.09	-1.03
TDRD7	**1.79**	**2.26**	1.22	1.07	APLP1	1.10	**1.28**	-1.08	1.02
SQRDL	**1.79**	1.16	**1.58**	1.12	TBX15	1.10	**1.26**	-1.05	1.01
TTC39B	**1.78**	**1.48**	**1.39**	1.17	NLRC5	1.09	**1.81**	-1.07	1.01
ZBED5-AS1	**1.78**	1.02	1.28	1.42	C6orf62	1.09	**1.18**	-1.03	-1.01
MSX1	**1.77**	**1.45**	1.36	1.13	ATP10A	1.08	**1.61**	1.06	1.08
CDK5R2	**1.76**	1.26	1.10	-1.04	ZGLP1	1.06	1.06	**1.82**	1.41
IFI35	**1.74**	**2.34**	-1.07	1.01	S1PR3	1.06	**1.25**	-1.06	1.08
EIF2AK2	**1.73**	**2.56**	1.03	-1.08	ETV6	1.06	**1.20**	1.01	1.05
HIP1R	**1.73**	1.00	1.37	1.04	RICTOR	1.05	**1.29**	1.10	1.06
PML	**1.71**	**2.05**	1.02	1.01	ANKFY1	1.05	**1.26**	1.01	-1.00
SIX1	**1.70**	1.24	1.14	-1.03	SOX9	1.05	**1.28**	**-1.29**	-1.13
TREX1	**1.69**	**1.77**	-1.04	-1.07	GNB4	1.05	**1.28**	-1.06	-1.05
FOXF1	**1.68**	1.07	**1.57**	1.09	BAZ1A	1.05	**1.24**	-1.00	1.00
CYP2J2	**1.67**	1.55	-1.15	-1.12	LOC100506714	1.04	1.28	1.25	**1.40**
ZFP42	**1.64**	**1.67**	1.10	1.17	ADAT2	1.04	-1.07	**1.55**	-1.00
NMI	**1.63**	**1.94**	1.10	-1.00	REEP2	1.04	1.15	**1.58**	1.27
SLAMF7	**1.63**	1.10	1.18	1.02	ZFP36	1.03	1.09	1.12	**1.22**
HIAT1	**1.62**	-1.03	1.17	-1.07	LETM2	1.02	-1.04	1.25	**1.41**
C18orf56	**1.62**	1.59	-1.43	-1.27	EBF4	-1.00	1.02	**3.36**	1.41
SPRY2	**1.62**	1.15	1.21	1.14	DCLRE1C	-1.00	**1.26**	-1.01	-1.06
IFI16	**1.60**	**1.96**	1.06	1.04	SLC30A4	-1.02	1.03	**1.25**	1.09
ZNF232	**1.60**	1.06	1.27	-1.25	KCNN3	-1.06	-1.05	**2.64**	**2.54**
SRGAP3	**1.59**	1.01	1.08	-1.00	INO80B	-1.06	-1.39	**1.92**	1.48
PIK3R3	**1.59**	1.07	**1.33**	-1.01	CDC14A	-1.09	-1.13	**1.30**	1.16
FZD4	**1.58**	-1.08	**1.55**	1.08	PHF10	-1.10	-1.10	**1.36**	1.09
VEGFC	**1.58**	1.18	1.32	1.05	ABCA3	-1.11	1.14	**5.12**	4.00
IRF2BPL	**1.58**	1.15	1.23	1.09	C4orf36	-1.13	-1.08	**1.65**	1.38
STAT1	**1.58**	**2.15**	-1.01	-1.01	AP1S3	-1.16	-1.02	1.23	**1.48**
TSKU	**1.57**	1.15	1.29	-1.04	LOC102724023	-1.17	1.84	**2.38**	1.24
GIMAP2	**1.57**	**1.57**	1.00	1.09	ADAMTS9	-1.19	-1.08	**1.92**	1.28
ZC3H12C	**1.56**	1.20	1.41	1.09	TMEM176A	-1.20	-1.22	1.43	**3.15**
PNP	**1.56**	1.06	1.33	1.03	OLFM4	-1.22	-1.10	**3.96**	-1.01
TRIM38	**1.54**	**1.80**	1.03	1.07	LOC100506258	-1.38	-1.08	2.22	**3.30**
IRF2	**1.52**	**1.55**	1.09	-1.00	NDP	-1.39	-1.67	**3.36**	1.43

Fold change calculated relative to mock infected wildtype or IFNAR KO cells

Values in bold are significantly different from mock

IFNAR: IFN-α/β receptor, HCMV-UV: UV-inactivated human cytomegalovirus, SeV-UV: UV-inactivated Sendai virus

Transparent Methods

Cells and viruses

Telomerized human fibroblasts (THFs) and THF IFNAR1 KOs (from Victor DeFilippis) were immortalized through expression of hTERT in BJ fibroblasts (Bresnahan et al., 2000). THF IRF3 KO and RelA KO were generated by transducing THF with lentivirus encoding Cas9 and gene specific gRNA, followed by selection of single cell clones lacking protein expression for the gene of interest. THF IFN-β-GFP cells were generated by transducing THF with lentivirus encoding green fluorescence protein (GFP) under the control of the IFN-β promoter region (Cellomics). Human embryonic lung (HEL) fibroblasts and NuLi-1 immortalized bronchiole epithelial cells were obtained from ATCC. THP-1 monocytes (from Dawn Bowdish) were differentiated into adherent macrophage-like cells by treatment with 100 nM PMA (Sigma-Aldrich) for 72 hours. SeV (Charles River) Cantell strain was produced in eggs and titred by plaque assay on CV-1 cells, HCMV strain AD169 (from Theresa Compton) was propagated and titred in human embryonic lung (HEL) fibroblasts and vesicular stomatitis virus expressing GFP (VSV-GFP) was propagated in Vero cells. Virus particles were counted by tunable resistive pulse sensing with a qViro-X particle counter (Izon). Virus inactivation was carried out in a stratolinker UV-crosslinker using working concentration of virus with the amount of energy optimized to yield a 5-log reduction in infectious titre. Treatments were done in minimal serum-free media for 1 hour at 37^{o}C with periodic rocking. E1000 dsDNA and dsRNA derived from the WNV genome was transcribed in vitro and purified as previously described (DeWitte-Orr et al., 2009). Transfections were carried out with lipofectamine 3000 (ThermoFisher) according to the manufacturer's instructions. B18R (Millipore) was used to block IFN at 50 ug/ml in serum-free media and incubated with cells for 30 minutes prior to treatment. Cycloheximide (Sigma) was used at 50 uM for a 30 minute pre-treatment and subsequent steps to inhibit protein synthesis.

Plaque reduction assay

Cells were conditioned with virus or other treatment and incubated 16 hours at 37^{o}C before challenge with VSV-GFP infection and an overlay containing 1% methyl-cellulose to restrict plaques. Immediately before VSV-GFP challenge, supernatants from treated cells were transferred to naive cells and allowed to sit for 6 hours before the supernatant conditioned cells

were also challenged with VSV-GFP. Plates were scanned with a Typhoon fluorescence scanner 24 hours post-infection with VSV-GFP to assay antiviral protection.

Transcriptome sequencing and analysis

RNA was extracted using an RNeasy RNA extraction kit (Qiagen) and treated with DNAase (Ambion) according to the manufacturer's instructions. cDNA libraries were created by polyA enrichment using NEBNext poly(A) magnetics isolation module (NEB) and reverse transcribed using NEBNext ultra II directional RNA library prep kit (NEB) according to the manufacturer's instructions. cDNA libraries were sequenced using an Illumina HiSeq rapid V2 (1 x 50 bp sequence reads) at the Farncombe Metagenomics Facility (McMaster University). Sequencing yielded ~1 x 10^7 reads/sample.

First, reads were filtered by quality (at least 90% of the bases must have a quality score of 20 and higher). Then the mapping of the remaining reads was performed using *HISAT2* (Kim et al., 2015) with hg38 (UCSC) reference genome; reads were counted by using *HTSeq count* (Anders et al., 2015). Genes showing less than 10 counts in more than 30% of the samples per group were removed using *filterByExpr* function in *EdgeR* package (McCarthy et al., 2012; Robinson et al., 2010) in R, resulting in 13,134 genes. These remaining count values were normalized with *TMM* normalization method (Robinson and Oshlack, 2010) and then transformed with *voom* transformation (Law et al., 2014). Next, batch effect was removed using ComBat (Johnson et al., 2007), with experiment date used as the batch information. *Limma* package (Ritchie et al., 2015) in R was used to examine differential expression between the groups of interest; p-values obtained from the analysis were corrected with BH correction for multiple testing (Benjamini and Hochberg, 1995), and corrected values <0.05 were considered to be significant.

Quantitative RT-PCR

RNA was extracted using TRIzol reagent (Invitrogen) or an RNeasy RNA extraction kit (Qiagen) and treated with DNAase (Ambion) according to the manufacturers' instructions. 500 ng of RNA was reversed transcribed using SuperScript II Reverse Transcriptase (Invitrogen) and random hexamer primers or with an iScript cDNA synthesis kit (BioRad) as per the manufacturer's instructions. Quantitative PCR reactions contained Taqman probes and Universal PCR Master Mix (Applied Biosystems) or primers and SsoFast EvaGreen Supermix (BioRad)

were used as indicated, along with PCR amplification on a StepOnePlus Q-PCR instrument (Applied Biosystems). Ct values were calculated and GAPDH was used as an endogenous control to calculate individual ΔΔCt values. ΔΔCt values of samples were compared with mock treated samples to calculate fold change. Taqman probes for human GAPDH (Hs02758991_g1), IFIT1 (Hs03027069_s1), ISG15 (Hs00192713_m1) and CXCL10 (Hs00171042_m1) and PCR primers for human GAPDH (F-5'-GGAGCGAGATCCCTCCAAAAT-3' and R-5'-GGCTGTTGTCATACTTCTCATGG-3'), genomic SeV (F-5'-GACCAGGAAATAAAGAGTGCA-3' and R-5'-CGATGTATTGGCATATAGCGT-3') and SeV DVG-546 (F-5'-TCCAAGACTATCTTTATCTATGTCC-3' and R-5'-GGTGAGGAATCTATACGTTATAC-3') were used.

Immunofluorescence

Cells were fixed on glass coverslips using 10% formalin, permeabilized in 0.2% Triton-X 100 in phosphate buffered saline (PBS) and blocked in 3% fetal bovine serum (FBS), 3% goat serum, 0.02% Tween-20 in PBS for 1 hour. The following antibodies were used for 1 hour at the indicated dilution in blocking buffer: anti-IRF3 (Millipore)(1:400), AlexaFluor488-conjugated anti-GFP (Invitrogen)(1:1000), anti-ISG15 (gift from Dr. EC Borden)(1:10), anti-SeV (1:2000), AlexaFluor488-conjugated anti-rabbit (Invitrogen)(1:400) and AlexaFluor594-conjugated anti-mouse (1:50). Hoechst 33258 (Invitrogen) was diluted 1:5000 in PBS and added to cells for 15 minutes. A Leica DM IRE2 microscope was used and IRF3 positive nuclei were calculated as a percentage of total nuclei using OpenLab software (Leica).

Flow cytometry

Cells were fixed and permeabilized using a cytofix/cytoperm fixation/permeabilization kit (BD Biosciences) according to the manufacturer's instructions. Cells were stained with anti-ISG15 (diluted 1:10) and APC-conjugated anti-mouse (Biolegend) (diluted 1:400) for 30 minutes each in perm/wash buffer (BD Biosciences). Flow cytometry of fixed cells was carried out in 1% BSA, 5mM EDTA in PBS using a MoFlow XDP cell sorter (Beckman Coulter). Cell populations were analyzed using FlowJo.

Supplemental References

Anders, S., Pyl, P.T., and Huber, W. (2015). HTSeq--a Python framework to work with high-throughput sequencing data. Bioinformatics *31*, 166-169.

Benjamini, Y., and Hochberg, Y. (1995). Controlling the false discovery rate: a practical and powerful approach to multiple testing. J R Statist Soc B *57*, 289-300.

Bresnahan, W.A., Hultman, G.E., and Shenk, T. (2000). Replication of wildtype and mutant human cytomegalovirus in life-extended human diploid fibroblasts. J Virol *74*, 10816-10818.

DeWitte-Orr, S.J., Mehta, D.R., Collins, S.E., Suthar, M.S., Gale, M., Jr., and Mossman, K.L. (2009). Long double-stranded RNA induces an antiviral response independent of IFN regulatory factor 3, IFN-beta promoter stimulator 1, and IFN. J Immunol *183*, 6545-6553.

Johnson, W.E., Li, C., and Rabinovic, A. (2007). Adjusting batch effects in microarray expression data using empirical Bayes methods. Biostatistics *8*, 118-127.

Kim, D., Langmead, B., and Salzberg, S.L. (2015). HISAT: a fast spliced aligner with low memory requirements. Nat Methods *12*, 357-360.

Law, C.W., Chen, Y., Shi, W., and Smyth, G.K. (2014). voom: Precision weights unlock linear model analysis tools for RNA-seq read counts. Genome Biol *15*, R29.

McCarthy, D.J., Chen, Y., and Smyth, G.K. (2012). Differential expression analysis of multifactor RNA-Seq experiments with respect to biological variation. Nucleic Acids Res *40*, 4288-4297.

Ritchie, M.E., Phipson, B., Wu, D., Hu, Y., Law, C.W., Shi, W., and Smyth, G.K. (2015). limma powers differential expression analyses for RNA-sequencing and microarray studies. Nucleic Acids Res *43*, e47.

Robinson, M.D., McCarthy, D.J., and Smyth, G.K. (2010). edgeR: a Bioconductor package for differential expression analysis of digital gene expression data. Bioinformatics *26*, 139-140.

Robinson, M.D., and Oshlack, A. (2010). A scaling normalization method for differential expression analysis of RNA-seq data. Genome Biol *11*, R25.